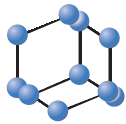


## OPINION ARTICLE


**BENTHAM  
SCIENCE**

# Could Small Neurotoxins-Peptides be Expressed during SARS-CoV-2 Infection?



Concetta Cafiero<sup>1,\*</sup>, Alessandra Micera<sup>2,\*</sup>, Agnese Re<sup>3</sup>, Loredana Postiglione<sup>4</sup>, Andrea Cacciamani<sup>2</sup>, Beniamino Schiavone<sup>5</sup>, Giulio Benincasa<sup>6</sup> and Raffaele Palmirotta<sup>7</sup>

<sup>1</sup>Medical Oncology, SG Moscati Hospital, Taranto, Italy; <sup>2</sup>Research Laboratories in Ophthalmology, IRCCS - Fondazione Bietti, Rome, Italy; <sup>3</sup>Department of Chemistry and Clinical Biochemistry, Catholic University of Sacred Heart, Fondazione Policlinico Universitario Agostino Gemelli IRCCS, Rome, Italy; <sup>4</sup>Department of Translational Medical Sciences, University of Federico II, Naples, Italy; <sup>5</sup>General Management Unit, Pineta Grande Hospital, Castel Volturno (CE), Italy; <sup>6</sup>Department of Clinical Pathology and Molecular Biology, Pineta Grande Hospital, Castel Volturno, (CE), Italy; <sup>7</sup>Interdisciplinary Department of Medicine, University of Bari 'Aldo Moro', School of Medicine, Bari, Italy

## ARTICLE HISTORY

Received: October 26, 2021  
Revised: October 30, 2021  
Accepted: December 08, 2021

DOI:  
10.2174/138920292366621122111527



CrossMark

This is an Open Access article published under CC BY 4.0  
<https://creativecommons.org/licenses/by/4.0/legalcode>

**Abstract:** SARS-CoV-2 pathogenesis has been recently extended to human central nervous system (CNS), in addition to nasopharyngeal truck, eye, lung and gut. The recent literature highlights that some SARS-CoV-2 spike glycoprotein regions homologous to neurotoxin-like peptides might bind to human nicotinic Acetyl-Choline Receptors (nAChRs). Spike-nAChR interaction can probably cause dysregulation of CNS and cholinergic anti-inflammatory pathways and uncontrolled immune-response, both associated to a severe COVID-19 pathophysiology. Herein, we hypothesize that inside the Open Reading Frame (ORF) region of spike glycoprotein, the RNA polymerase can translate small neurotoxic peptides by means of a “jumping mechanism” already demonstrated in other coronaviruses. These small peptides can bind the snAChRs instead of Spike glycoproteins. A striking homology occurred between these small peptides observed by sequence retrieval and proteins alignment. Acting as nAChRs antagonists, these small peptides (conotoxins) could be the explanation for the extrapulmonary clinical manifestations (neurological, hemorrhagic and thrombotic expressions, the prolonged apnea, the cardiocirculatory collapse, the heart arrhythmias, the ventricular tachycardia, the body temperature alteration, the electrolyte K<sup>+</sup> imbalance and finally the significant reduction of butyryl cholinesterase (BuChE) plasma levels, as observed in COVID-19 patients. Several factors might induce the expression of these small peptides, including microbiota. The main hypothesis regarding the presence of these small peptides opens a new scenario on the etiology of COVID-19 clinical symptoms observed so far, including the neurological manifestations.

**Keywords:** SARS-CoV-2 genome, infection, neurotoxins, acetylcholine, sequence alignment, microbiome.

## 1. INTRODUCTION

The COVID-19 pandemic, a global emergency due to SARS-CoV-2 infection, has resulted in 187,827,660 confirmed cases of infection and 4,055,497 deaths from beginning to date (World Health Organization - WHO) [1]. The presence of previous chronic diseases represents a significant risk factor and influences the prognosis as making patients more vulnerable to COVID-19 disease, from progression towards worsening outcomes [2]. In addition, other lifestyle-related risk factors such as physical inactivity, obesity, excessive alcohol intake and smoking, have also been proposed [3, 4].

Particular attention has been devoted to smoking, as evidence indicate that smokers with COVID-19 are more likely

to have serious illness and adverse outcomes once hospitalized [5]. However, the number of smokers requiring hospitalization is far lower than expected, according to population smoking rates [5, 6-9]. Since the beginning of the pandemic, several studies have shown a negative association between smoking prevalence and COVID-19 hospitalized patients, leading some researchers to hypothesize a possible therapeutic role of nicotine in the course of SARS-CoV-2 infection [7, 10, 11].

Based on these observations, some research groups have suggested an interaction between the human nicotinic acetylcholine receptor (nAChRs) and SARS-CoV-2virus, in line with the finding that viral Spike glycoprotein has specific motifs related to known nAChR antagonists [5, 7, 8, 11].

SARS-CoV-2 virus, initially isolated from ocular secretions of COVID-19 affected patients [12], is part of β-coronaviruses' group and contains a single-stranded positive RNA (~29.9kB) with 14 Open Reading Frames (ORFs) encoding for 27 different proteins [13, 14]. Spike glycoprotein is expressed on the surface of virus envelope, representing a fun-

\*Address correspondence to this author at the Medical Oncology, SG Moscati Hospital, Taranto, Italy; E-mail: [concettacafiero@gmail.com](mailto:concettacafiero@gmail.com); Research Laboratories in Ophthalmology, IRCCS - Fondazione Bietti, Rome, Italy; E-mail: [alessandra.micera@fondazionebietti.it](mailto:alessandra.micera@fondazionebietti.it)  
<sup>†</sup>These authors contributed equally to this work and share first authorship.

damental key point to mediate the entry of SARS-CoV-2 into host cells by recognition of human ACE2 (hACE2) receptor through a region defined as Receptor-Binding Domain (RBD) [15, 16].

Using a molecular dynamics computer simulation based on data from a previous study by Changeux and coworkers, Oliveira and coworkers identified i. a region on Spike protein ranging from amino acids 674 to 685 with high homology to several neurotoxins as  $\alpha$ -bungarotoxin, a nAChR antagonist directly competing with acetylcholine identified in the snake *Bungarus multicinctus*, and ii. a high affinity region for the human  $\alpha 4\beta 2$  and  $\alpha 7$ -nAChR subtypes [8, 11]. The same research team also hypothesized the interaction of spike protein with  $\alpha 7$ -nAChR [8, 11].

By sequence alignments, Farsalinos and coworkers identified homology between the Spike Glycoprotein area between the aa 375-390 and the neurotoxin homolog NL1. This *in-silico* study suggested a strong interaction of the amino acid motif with the nAChR  $\alpha 9$  subunit [17]. The aa 375-390 peptide fragment is included in the RBD spanning aa 319-541, a domain that enables the spike protein to recognize ACE2 on the host cells [17]. Further advanced *in-silico* studies by the same group highlighted that the sequence of the aa 375-390 corresponded with the previously described cryptic epitope for human anti-SARS-CoV antibody CR3022, and through a particular and unusual folding of Spike glycoprotein, it might also bind to  $\alpha 7$ -nAChR [6].

The involvement of the nicotinic cholinergic system might explain some aspects of COVID-19 pathogenesis not well understood to date. Numerous evidence suggests a neurotropic action of SARS-CoV-2, a point also confirmed by a recent study in which it was demonstrated how the virus could penetrate through the olfactory mucosa and follow the neuro-anatomical structures reaching the primary respiratory and cardiovascular control centers of the medulla oblongata [18]. Retrospective studies have demonstrated neurological manifestations in more than 30% of COVID-19 patients with Central Nervous System (CNS) symptoms such as dizziness, headache, impaired consciousness, acute cerebrovascular disease, ataxia, and seizure, in addition to the loss of smell and taste that are specific to this disease [19].

Activation of  $\alpha 7$ -nAChRs, particularly expressed by B cells, T cells, and macrophages, reduces the production of proinflammatory cytokines such as interleukin-1 (IL-1), interleukin-6 (IL-6), interleukin-8 (IL-8) and tumor necrosis factor- $\alpha$  (TNF- $\alpha$ ) through a “cholinergic anti-inflammatory pathway” triggered by nicotine or nicotinic agonists [9, 20]. This nAChR antagonistic action of virus would therefore explain the “cytokine storm” and the hyperinflammatory syndrome observed in several COVID-19 patients [9, 11]. Numerous authors also hypothesized a prominent role of macrophages highlighting that the antagonistic action on  $\alpha 7$ -nAChRs by SARS-CoV-2 determines a dysregulation of the polarization mechanism and a permanence of M1 type macrophages, with a consequent increase in the concentration of inflammatory cytokines [21].

Finally, it is interesting to note that  $\alpha 7$ -nAChRs are also present on the surface of platelets and that, as previously demonstrated, their inhibition can lead to an increase in their activity and consequent clot formation, thus explaining coagulopathy and thrombus formation in COVID-19 patients [9, 11].

Recently, the direct effect of inhibition of COVID-19 on critical survival genes has also been hypothesized, such as Sirt 1, that are linked to expression levels of  $\alpha 7$ -nAChRs [22, 23], resulting in effects that can range from inflammatory processes to programmed cell death [24].

## 2. SEQUENCE ALIGNMENT ANALYSIS

We mainly focused on the previously mentioned alignment studies that demonstrated a sequence homology between some regions of the virus Spike glycoprotein and nAChR antagonists such as  $\alpha$ -bungarotoxin [8, 11] and Neurotoxin homolog NL1 [5, 6].

To verify the similarity between SARS-CoV-2 Spike glycoprotein sequence [6] and different neurotoxins with nAChR antagonistic action, we used EMBOSS Needle, a bioinformatic sequence analysis application provided by European Molecular Biology Laboratory - European Bioinformatics Institute (EMBL-EBI) ([https://www.ebi.ac.uk/Tools/psa/emboss\\_needle/](https://www.ebi.ac.uk/Tools/psa/emboss_needle/)) [25, 26].

EMBOSS, acronym for European Molecular Biology Open Software Suite, is a free open-source software analysis package and contains a wide array of general-purpose bioinformatics programs for the needs of the molecular biology user community. Among these, EMBOSS Needle tool reads and compares two input sequences along with their entire length and writes their optimal global sequence alignment to file. The software uses the Needleman-Wunsch alignment algorithm, an automatic procedure for calculating the best possible alignment between two amino acid sequences [27]. This method allows to perform a fast and ingenious comparison between all the alignments among two sequences, considering every possible number of gaps in every possible position. Software's purpose is to choose the best alignment among all produced, simply the one that guarantees the highest 'score'. A short description of the steps used by this tool and an example of the output file are reported in Supplementary Fig. (1). Moreover, it is possible to view the entire procedure used by the software at [https://www.youtube.com/watch?v=\\_1m1WOOuv5o&t=67s](https://www.youtube.com/watch?v=_1m1WOOuv5o&t=67s) [28]. First, we performed a protein alignment between the 1273 aa SARS-CoV-2 spike glycoprotein (NCBI Gene ID: NC\_045512.2) [14] and the mentioned above Neurotoxin homolog NL1 (UniProtKB - Q9DEQ3 - 3SO8\_NAJAT), a polypeptide of 86 aa identified in *Najaatra* (Chinese cobra) [5, 6]. We noted that the presence of identical or functionally equivalent amino acids is not limited to the 375-390 region, as previously described, but it is also present in other areas of the Spike glycoprotein with a sequence homology of 47/86 aa (54.6%) (Fig. 1, Supplementary Table 1). Interestingly, we also found homology for the Muscarinic toxin-like protein, identified in *Bungarus multicinctus* (Many-banded krait; UniPro

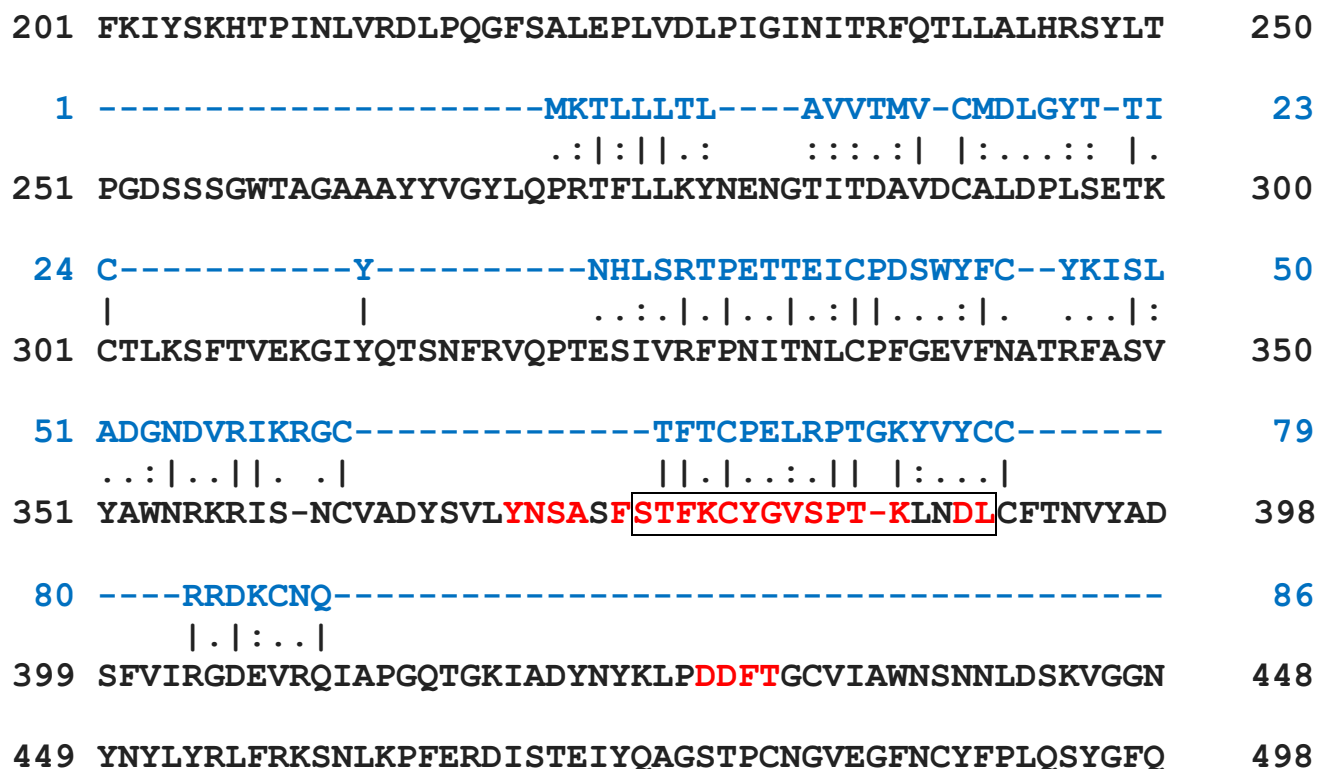


**Fig. (1).** Protein Sequence Alignment performed using EMBOSS Needle between SARS-CoV-2 Spike glycoprotein (GenBank: NC\_045512.2) and Neurotoxin homolog NL1, Najaatra (Chinese cobra) (UniProtKB - Q9DEQ3 - 3SO8\_NAJAT) protein. Black: Spike protein. Blue: Conotoxin proteins. Red: SARS-CoV-2 RBD epitope sequence for the CR3022 mAb. Framework: highly conserved region of SARS-CoVs’ RBD (375–395 aa). (|): identities, (:): conservative replacements, (.) : non-conservative replacements. (A higher resolution / colour version of this figure is available in the electronic copy of the article).

tKB: Q9W727 - 3SO8\_BUNMU), which exhibits an entirely similar sequence to Neurotoxin homolog NL1. Furthermore, we found a homology between the cryptic epitope for the human antibody CR3022 and the 27 aa Kappa-conotoxin-like as14a, identified in *Conus cancellatus* (Cancellate cone; *Conus austini*; UniProtKB: P0C6S2 - CLEA\_CONCF), with an overall sequence homology of 12/27 aa (44.4%) (Supplementary Table 1). Later, we proceeded to find several conotoxins protein sequences from the UniProt Knowledgebase (UniProtKB) database (<https://www.uniprot.org/uniprot/>) [29] and always carrying out alignment with SARS-CoV-2 Spike glycoprotein. In all cases, we found a certain rate of homology with the Spike glycoprotein also in regions different from the cryptic epitope for the human antibody CR3022 and with percentages of homology ranging from 22.7% to 50.8%, with an average of 37% (Supplementary Table 1).

Our *in-silico* analysis, through sequence retrieval and protein alignment, shows high positive correlation between small genome regions and different toxins, like conotoxin, that selectively could interact with nAChRs. Being nAChR antagonists, these toxins are used by cone snails to immobilize their prey [30]. The release of (oligo-) peptides almost identical to animal conotoxins could result in clinical mani-

festations such as neurological, hemorrhagic and thrombotic. This expression would explain the presence of symptoms of COVID-19 pathogenesis not yet fully clarified, such as prolonged apnea, cardiocirculatory collapse, heart arrhythmias, ventricular tachycardia, body temperature alteration, electrolyte imbalance (particularly K<sup>+</sup>) and even the significant reduction of butyrylcholinesterase (BuChE) plasma levels.

Thus, the data obtained from our analyses indicate that regions of homology with neurotoxin-like peptides are more numerous and more widely distributed on the Spike glycoprotein than previously observed by others [31].

### 3. DISCUSSION

Based on these high levels of homology, we hypothesize that inside the last ORF of viral genome encoding for Spike glycoprotein, the RNA polymerase can encode these small proteins. This hypothesis is supported by several pieces of evidence reporting that SARS-CoV-2 viral RNA polymerase, through a “jumping mechanism” already demonstrated in the other coronavirus, results in numerous discontinuous transcription events, which are likely to include small neurotoxin-like proteins such as conotoxins [32, 33]. Indeed,

while the role of many structural SARS-CoV-2 proteins is well described in the literature, several sgRNAs encoded by RNA polymerase jumping unusual display structure and a still unknown function [34]. The inhibition of AChRs can play a central role in cholinergic CNS and PNS synapses [11] and particularly the AChRs:nicotine binding might block nAChRs, supporting the hypothesis of a protective role for nicotine and other cholinergic agonists, in line with the observation that smokers are almost “protected” against SARS-CoV-2 hospitalization [17, 19, 35]. The absence of nAChRs:nicotine binding could provide logical explanations for acute inflammatory disorder in these patients, as COVID-19 pathology may be linked to severe dysregulation of CNS [10]. Finally, this hypothesis could explain the detection of some toxic products into bloodstream and tissues [36] and the correlation between different taxa compositions of nasopharyngeal or gastrointestinal microbiota and the severity of COVID-19 disease [37].

Certainly, the hypothesis of synthesis of small neurotoxic peptide herein described opens a new scenario on the etiology of COVID-19 clinical symptoms observed so far, including the neurological manifestations. Indeed, the presence of conotoxins-like peptides could explain the appearance of many symptoms including hyposmia, hypogeusia and the typical signs of Guillain Barre syndrome observed in some patients with COVID-19 [38]. As stated, the presence of toxic peptides can alter the normal functioning of ion channels, nicotinic AChR as well as ACh levels and induce a significant reduction of plasmatic BuChE levels [39].

However, the reason for production of these oligopeptides binding to nAChR still remains poorly understood and many doubts remain about the mechanisms related to transcriptional processes of the virus [33, 40]. The above-mentioned literature on computational modeling suggested that SARS-CoV-2 spike glycoprotein might bind to nAChRs by a particular and unusual folding, also through a cryptic epitope that coincides with the well-described cryptic epitope for the human SARS-CoV antibody CR3022 [5, 6, 8, 11]. By the way, it is well known that these peptides are functional macromolecules characterized by a specific 3D “native” structure that allows their functions correctly, once at final conformation [41]. The reaching of the final 3D-folding stability is assisted by specific protein complexes (chaperones) that guarantee the conservation of protein functions [41, 42]. Therefore, it is strongly unlikely that Spike protein, specifically a 1273 aa large protein, can totally change its folding to express a small peptide portion of 30 aa able to bind the nicotinic receptor [6]. We strongly support the hypothesis that, through a “jumping mechanism” [33, 40], the RNA polymerase can prime the transcription of small peptides, like conotoxins, whose sequence is contained in the ORF region encoding for Spike glycoprotein. This possibility could be primed by external biological factors such as the host's microbiota [43]. Indeed, recent studies identified a different microbiome depending on ageing and their tissue distribution (gut, lung and eye), allowing us to hypothesize that microbiota can play a crucial role in directing the expression of this small protein by SARS-CoV-2 [32, 43-45]. As observed in COVID-19, elderly subjects are affected by more severe

forms of disease, and most probably COVID-19 disease worsens in younger in the presence of dysbiosis and/or when certain bacterial taxonomies prevail [46-50]. In this context, it is interesting the hypothesis recently proposed that bacterial lipopolysaccharides (LPS) may repress sirt 1 with a consequent effect on nAChRs resulting in a greater severity of covid-19 infection in elderly individuals [24].

Therefore, the microbiome, belonging to specific body districts, represents a valuable “new entry” in the biomedical and therapeutical fields for COVID-19 patients [40, 46, 50].

## CONCLUSION

In view of the above reported considerations, some therapeutic solutions can be prospected. First, we must consider that conus venom is highly toxic and lethal as it is composed of many different types of conotoxins ( $\alpha$ ,  $\delta$ ,  $\kappa$ ,  $\mu$  and  $\omega$ ) which have neurological effects, due to different receptor targets [51, 52]. Indeed, the conotoxins are generally weakly immunogenic and therefore, not effectively targeted by current polyclonal anti-venom therapies [53]. Although the use of monoclonal anti-toxin directed either towards the virus surface antigens and/or the released virus products could be a quick solution to reduce mortality rates, it remains difficult to apply. On the contrary, nAChR can bind these toxins and therefore, it can be used against neurotoxic envenoming [53-56]. The administration of cholinesterase-derived human BuChE could be hypothesized as a potential therapeutic approach [51]. On the other hand, a therapeutic approach using nAChRs agonists, as hypothesized by a previous *in silico* study, cannot be ruled out [10].

Undoubtedly, our hypothesis remains to be proven and numerous efforts still need to be made by researchers to eradicate this serious pandemic that is affecting health and the economy globally.

## LIST OF ABBREVIATIONS

hACE2	= human Angiotensin-Converting Enzyme 2
CNS	= central Nervous System
nAChRs	= nicotinic Acetyl-Choline Receptors
ORF	= Open Reading Frame
BuChE	= butyryl Cholinesterase
WHO	= World Health Organization
RBD	= Receptor-Binding Domain
IL-1	= interleukin-1
IL-6	= interleukin-6
IL-8	= interleukin-8
SIRT1	= Sirtuin 1
TNF- $\alpha$	= Tumor Necrosis Factor- $\alpha$
EMBL-EBI	= European Molecular Biology Laboratory - European Bioinformatics Institute

EMBOSS = European Molecular Biology Open Software Suite

**CONSENT FOR PUBLICATION**

Not applicable.

**FUNDING**

None.

**CONFLICT OF INTEREST**

The authors declare no conflict of interest, financial or otherwise.

**ACKNOWLEDGEMENTS**

AM and AC are supported by Ministry of Health and Fondazione Roma.

**SUPPLEMENTARY MATERIAL**

Supplementary material is available on the publisher’s website along with the published article.

**REFERENCES**

[1] World Health Organization (WHO). WHO Coronavirus (COVID-19) Dashboard. Geneva: WHO. Available from: <https://covid19.who.int> Accessed, July 15, 2021

[2] Wang, D.; Hu, B.; Hu, C.; Zhu, F.; Liu, X.; Zhang, J.; Wang, B.; Xiang, H.; Cheng, Z.; Xiong, Y.; Zhao, Y.; Li, Y.; Wang, X.; Peng, Z. Clinical characteristics of 138 hospitalized patients with 2019 novel coronavirus-infected pneumonia in Wuhan, China. *JAMA*, **2020**, *323*(11), 1061-1069. <http://dx.doi.org/10.1001/jama.2020.1585> PMID: 32031570

[3] Lassen, M.C.H.; Skaarup, K.G.; Sengelov, M.; Iversen, K.; Ulrik, C.S.; Jensen, J.U.S.; Biering-Sørensen, T. Alcohol consumption and the risk of acute respiratory distress syndrome in COVID-19. *Ann. Am. Thorac. Soc.*, **2021**, *18*(6), 1074-1076. <http://dx.doi.org/10.1513/AnnalsATS.202008-988RL> PMID: 33315543

[4] Hamer, M.; Kivimäki, M.; Gale, C.R.; Batty, G.D. Lifestyle risk factors, inflammatory mechanisms, and COVID-19 hospitalization: A community-based cohort study of 387,109 adults in UK. *Brain Behav. Immun.*, **2020**, *87*, 184-187. <http://dx.doi.org/10.1016/j.bbi.2020.05.059> PMID: 32454138

[5] Farsalinos, K.; Angelopoulou, A.; Alexandris, N.; Poulas, K. COVID-19 and the nicotinic cholinergic system. *Eur. Respir. J.*, **2020**, *56*(1), 2001589. <http://dx.doi.org/10.1183/13993003.01589-2020> PMID: 32444400

[6] Lagoumintzis, G.; Chasapis, C.T.; Alexandris, N.; Kouretas, D.; Tzartos, S.; Eliopoulos, E.; Farsalinos, K.; Poulas, K. Nicotinic cholinergic system and COVID-19: *In silico* identification of interactions between  $\alpha 7$  nicotinic acetylcholine receptor and the cryptic epitopes of SARS-CoV and SARS-CoV-2 spike glycoproteins. *Food Chem. Toxicol.*, **2021**, *149*, 112009. <http://dx.doi.org/10.1016/j.fct.2021.112009> PMID: 33503469

[7] Farsalinos, K.; Eliopoulos, E.; Leonidas, D.D.; Papadopoulos, G.E.; Tzartos, S.; Poulas, K. Nicotinic cholinergic system and COVID-19: *In silico* identification of an interaction between SARS-CoV-2 and nicotinic receptors with potential therapeutic targeting implications. *Int. J. Mol. Sci.*, **2020**, *21*(16), 5807. <http://dx.doi.org/10.3390/ijms21165807> PMID: 32823591

[8] Oliveira, A.S.F.; Ibarra, A.A.; Bermudez, I.; Casalino, L.; Gaieb, Z.; Shoemark, D.K.; Gallagher, T.; Sessions, R.B.; Amaro, R.E.; Mulholland, A.J. A potential interaction between the SARS-CoV-2 spike protein and nicotinic acetylcholine receptors. *Biophys. J.*, **2021**, *120*(6), 983-993.

[9] <http://dx.doi.org/10.1016/j.bj.2021.01.037> PMID: 33609494  
Tizabi, Y.; Getachew, B.; Copeland, R.L.; Aschner, M. Nicotine and the nicotinic cholinergic system in COVID-19. *FEBS J.*, **2020**, *287*(17), 3656-3663.

[10] <http://dx.doi.org/10.1111/febs.15521> PMID: 32790936  
Alexandris, N.; Lagoumintzis, G.; Chasapis, C.T.; Leonidas, D.D.; Papadopoulos, G.E.; Tzartos, S.J.; Tsatsakis, A.; Eliopoulos, E.; Poulas, K.; Farsalinos, K. Nicotinic cholinergic system and COVID-19: *In silico* evaluation of nicotinic acetylcholine receptor agonists as potential therapeutic interventions. *Toxicol. Rep.*, **2020**, *8*, 73-83. <http://dx.doi.org/10.1016/j.toxrep.2020.12.013> PMID: 33425684

[11] Changeux, J.P. Discovery of the first neurotransmitter receptor: The acetylcholine nicotinic receptor. *Biomolecules*, **2020**, *10*(4), 547. <http://dx.doi.org/10.3390/biom10040547> PMID: 32260196

[12] Colavita, F.; Lapa, D.; Carletti, F.; Lalle, E.; Bordini, L.; Marsella, P.; Nicastrì, E.; Bevilacqua, N.; Giancola, M.L.; Corpolongo, A.; Ippolito, G.; Capobianchi, M.R.; Castilletti, C. SARS-CoV-2 isolation from ocular secretions of a patient with COVID-19 in Italy with prolonged viral RNA detection. *Ann. Intern. Med.*, **2020**, *173*(3), 242-243. <http://dx.doi.org/10.7326/M20-1176> PMID: 32302380

[13] V'kovski, P.; Kratzel, A.; Steiner, S.; Stalder, H.; Thiel, V. Coronavirus biology and replication: Implications for SARS-CoV-2. *Nat. Rev. Microbiol.*, **2021**, *19*(3), 155-170. <http://dx.doi.org/10.1038/s41579-020-00468-6> PMID: 33116300

[14] Wu, A.; Peng, Y.; Huang, B.; Ding, X.; Wang, X.; Niu, P.; Meng, J.; Zhu, Z.; Zhang, Z.; Wang, J.; Sheng, J.; Quan, L.; Xia, Z.; Tan, W.; Cheng, G.; Jiang, T. Genome composition and divergence of the novel coronavirus (2019-nCoV) originating in China. *Cell Host Microbe*, **2020**, *27*(3), 325-328. <http://dx.doi.org/10.1016/j.chom.2020.02.001> PMID: 32035028

[15] Shang, J.; Wan, Y.; Luo, C.; Ye, G.; Geng, Q.; Auerbach, A.; Li, F. Cell entry mechanisms of SARS-CoV-2. *Proc. Natl. Acad. Sci. USA*, **2020**, *117*(21), 11727-11734. <http://dx.doi.org/10.1073/pnas.2003138117> PMID: 32376634

[16] Cafiero, C.; Rosapepe, F.; Palmirota, R.; Re, A.; Ottaiano, M.P.; Benincasa, G.; Perone, R.; Varriale, E.; D'Amato, G.; Cacciamani, A.; Micera, A.; Pisconti, S. Angiotensin system polymorphisms in SARS-CoV-2 positive patients: Assessment between symptomatic and asymptomatic patients: A pilot study. *Pharm. Genomics Pers. Med.*, **2021**, *14*, 621-629. <http://dx.doi.org/10.2147/PGPM.S303666> PMID: 34079337

[17] Farsalinos, K.; Niaura, R.; Le Houezec, J.; Barbouni, A.; Tsatsakis, A.; Kouretas, D.; Vantarakis, A.; Poulas, K. Editorial: Nicotine and SARS-CoV-2: COVID-19 may be a disease of the nicotinic cholinergic system. *Toxicol. Rep.*, **2020**, *7*, 658-663. <http://dx.doi.org/10.1016/j.toxrep.2020.04.012> PMID: 32355638

[18] Meinhardt, J.; Radke, J.; Dittmayer, C.; Franz, J.; Thomas, C.; Mothes, R.; Laue, M.; Schneider, J.; Brünink, S.; Greuel, S.; Lehmann, M.; Hassan, O.; Aschman, T.; Schumann, E.; Chua, R.L.; Conrad, C.; Eils, R.; Stenzel, W.; Windgassen, M.; Rößler, L.; Goebel, H.H.; Gelderblom, H.R.; Martin, H.; Nitsche, A.; Schulz-Schaeffer, W.J.; Hakroush, S.; Winkler, M.S.; Tampe, B.; Scheibe, F.; Körtvélyessy, P.; Reinhold, D.; Siegmund, B.; Kühl, A.A.; Elezkurtaj, S.; Horst, D.; Oesterhelweg, L.; Tsokos, M.; Inggold-Heppner, B.; Stadelmann, C.; Drost, C.; Corman, V.M.; Radbruch, H.; Heppner, F.L. Olfactory transmucosal SARS-CoV-2 invasion as a port of central nervous system entry in individuals with COVID-19. *Nat. Neurosci.*, **2021**, *24*(2), 168-175. <http://dx.doi.org/10.1038/s41593-020-00758-5> PMID: 33257876

[19] Mao, L.; Jin, H.; Wang, M.; Hu, Y.; Chen, S.; He, Q.; Chang, J.; Hong, C.; Zhou, Y.; Wang, D.; Miao, X.; Li, Y.; Hu, B. Neurologic manifestations of hospitalized patients with coronavirus disease 2019 in Wuhan, China. *JAMA Neurol.*, **2020**, *77*(6), 683-690. <http://dx.doi.org/10.1001/jamaneurol.2020.1127> PMID: 32275288

[20] Changeux, J.P.; Amoura, Z.; Rey, F.A.; Miyara, M. A nicotinic hypothesis for Covid-19 with preventive and therapeutic implications. *C. R. Biol.*, **2020**, *343*(1), 33-39. PMID: 32720486

[21] Tanmay, S.; Labrou, D.; Farsalinos, K.; Poulas, K. Is SARS-CoV-2 Spike glycoprotein impairing macrophage function via  $\alpha 7$ -nico-

- tinic acetylcholine receptors? *Food Chem. Toxicol.*, **2021**, *152*, 112184.  
<http://dx.doi.org/10.1016/j.fct.2021.112184> PMID: 33838172
- [22] Huarachi Olivera, R.E.; Lazarte Rivera, A. Coronavirus disease (COVID-19) and sirtuins. *Rev. Fac. Cien. Med. Univ. Nac. Cordoba*, **2020**, *77*(2), 117-125.  
<http://dx.doi.org/10.31053/1853.0605.v77.n2.28196> PMID: 32558516
- [23] Cao, K.; Dong, Y.T.; Xiang, J.; Xu, Y.; Li, Y.; Song, H.; Yu, W.F.; Qi, X.L.; Guan, Z.Z. The neuroprotective effects of SIRT1 in mice carrying the APP/PS1 double-transgenic mutation and in SH-SY5Y cells over-expressing human APP670/671 may involve elevated levels of  $\alpha 7$  nicotinic acetylcholine receptors. *Aging (Albany NY)*, **2020**, *12*(2), 1792-1807.  
<http://dx.doi.org/10.18632/aging.102713> PMID: 32003755
- [24] Martins, I.J. Infection and anti-aging gene inactivation. *Acta Sci. Nutr Health*, **2020**, *4*, 01-02.
- [25] Madeira, F.; Park, Y.M.; Lee, J.; Buso, N.; Gur, T.; Madhusoodanan, N.; Basutkar, P.; Tivey, A.R.N.; Potter, S.C.; Finn, R.D.; Lopez, R. The EMBL-EBI search and sequence analysis tools APIs in 2019. *Nucleic Acids Res.*, **2019**, *47*(W1), W636-W641.  
<http://dx.doi.org/10.1093/nar/gkz268> PMID: 30976793
- [26] EMBOSS Needle. Available from: [https://www.ebi.ac.uk/Tools/pa-sa/emboss\\_needle/](https://www.ebi.ac.uk/Tools/pa-sa/emboss_needle/) (Accessed, July 15, 2021).
- [27] Needleman, S.B.; Wunsch, C.D. A general method applicable to the search for similarities in the amino acid sequence of two proteins. *J. Mol. Biol.*, **1970**, *48*(3), 443-453.  
[http://dx.doi.org/10.1016/0022-2836\(70\)90057-4](http://dx.doi.org/10.1016/0022-2836(70)90057-4) PMID: 5420325
- [28] Global Alignment Using EMBOSS Needle. Youtube. Available from: [https://www.youtube.com/watch?v=\\_lm1WOOuv5o&t=67s](https://www.youtube.com/watch?v=_lm1WOOuv5o&t=67s) (Accessed, December 5, 2021).
- [29] UniProt Knowledgebase (UniProtKB) database. Available from: <https://www.uniprot.org/uniprot/> Accessed, July 15, 2021
- [30] Becker, S.; Terlau, H. Toxins from cone snails: Properties, applications and biotechnological production. *Appl. Microbiol. Biotechnol.*, **2008**, *79*(1), 1-9.  
<http://dx.doi.org/10.1007/s00253-008-1385-6> PMID: 18340446
- [31] Mir, R.; Karim, S.; Kamal, M.A.; Wilson, C.M.; Mirza, Z. Conotoxins: Structure, therapeutic potential and pharmacological applications. *Curr. Pharm. Des.*, **2016**, *22*(5), 582-589.  
<http://dx.doi.org/10.2174/1381612822666151124234715> PMID: 26601961
- [32] Kim, S.; Jazwinski, S.M. The gut microbiota and healthy aging: A mini-review. *Gerontology*, **2018**, *64*(6), 513-520.  
<http://dx.doi.org/10.1159/000490615> PMID: 30025401
- [33] Sola, I.; Almazán, F.; Zúñiga, S.; Enjuanes, L. Continuous and discontinuous RNA synthesis in coronaviruses. *Annu. Rev. Virol.*, **2015**, *2*(1), 265-288.  
<http://dx.doi.org/10.1146/annurev-virology-100114-055218> PMID: 26958916
- [34] Romano, M.; Ruggiero, A.; Squeglia, F.; Maga, G.; Berisio, R. A structural view of SARS-CoV-2 RNA replication machinery: RNA synthesis, proofreading and final capping. *Cells*, **2020**, *9*(5), 1267.  
<http://dx.doi.org/10.3390/cells9051267> PMID: 32443810
- [35] van Westen-Lagerweij, N.A.; Meijer, E.; Meeuwse, E.G.; Chavannes, N.H.; Willemsen, M.C.; Croes, E.A. Are smokers protected against SARS-CoV-2 infection (COVID-19)? The origins of the myth. *NPJ Prim. Care Respir. Med.*, **2021**, *31*(1), 10.  
<http://dx.doi.org/10.1038/s41533-021-00223-1> PMID: 33637750
- [36] Li, C.X.; Chen, J.; Lv, S.K.; Li, J.H.; Li, L.L.; Hu, X. Whole-transcriptome RNA sequencing reveals significant differentially expressed mRNAs, miRNAs, and lncRNAs and related regulating biological pathways in the peripheral blood of COVID-19 patients. *Mediators Inflamm.*, **2021**, *2021*, 6635925.  
<http://dx.doi.org/10.1155/2021/6635925> PMID: 33833618
- [37] Brogna, B.; Brogna, C.; Petrillo, M.; Conte, A.M.; Benincasa, G.; Montano, L.; Piscopo, M. SARS-CoV-2 detection in fecal sample from a patient with typical findings of COVID-19 pneumonia on CT but negative to multiple SARS-CoV-2 RT-PCR tests on oropharyngeal and nasopharyngeal swab samples. *Medicina (Kaunas)*, **2021**, *57*(3), 290.  
<http://dx.doi.org/10.3390/medicina57030290> PMID: 33804646
- [38] Abdullahi, A.; Candan, S.A.; Soysal Tomruk, M.; Elibol, N.; Dada, O.; Truijen, S.; Saeyns, W. Is Guillain-Barré Syndrome associated with COVID-19 infection? A systemic review of the evidence. *Front. Neurol.*, **2021**, *11*, 566308.  
<http://dx.doi.org/10.3389/fneur.2020.566308> PMID: 33519663
- [39] Lebbe, E.K.; Peigneur, S.; Wijesekara, I.; Tytgat, J. Conotoxins targeting nicotinic acetylcholine receptors: An overview. *Mar. Drugs*, **2014**, *12*(5), 2970-3004.  
<http://dx.doi.org/10.3390/md12052970> PMID: 24857959
- [40] Kim, D.; Lee, J.Y.; Yang, J.S.; Kim, J.W.; Kim, V.N.; Chang, H. The architecture of SARS-CoV-2 transcriptome. *Cell*, **2020**, *181*(4), 914-921.e10.  
<http://dx.doi.org/10.1016/j.cell.2020.04.011> PMID: 32330414
- [41] Best, R.B. Race to the native state. *Proc. Natl. Acad. Sci. USA*, **2018**, *115*(10), 2267-2269.  
<http://dx.doi.org/10.1073/pnas.1722622115> PMID: 29472450
- [42] Englander, S.W.; Mayne, L. The nature of protein folding pathways. *Proc. Natl. Acad. Sci. USA*, **2014**, *111*(45), 15873-15880.  
<http://dx.doi.org/10.1073/pnas.1411798111> PMID: 25326421
- [43] Zhang, D.; Li, S.; Wang, N.; Tan, H.Y.; Zhang, Z.; Feng, Y. The cross-talk between gut microbiota and lungs in common lung diseases. *Front. Microbiol.*, **2020**, *11*, 301.  
<http://dx.doi.org/10.3389/fmicb.2020.00301> PMID: 32158441
- [44] Bischoff, S.C. Microbiota and aging. *Curr. Opin. Clin. Nutr. Metab. Care*, **2016**, *19*(1), 26-30.  
<http://dx.doi.org/10.1097/MCO.0000000000000242> PMID: 26560527
- [45] Li, J.J.; Yi, S.; Wei, L. Ocular microbiota and intraocular inflammation. *Front. Immunol.*, **2020**, *11*, 609765.  
<http://dx.doi.org/10.3389/fimmu.2020.609765> PMID: 33242865
- [46] Ventero, M.P.; Cuadrat, R.R.C.; Vidal, I.; Andrade, B.G.N.; Molina-Pardines, C.; Haro-Moreno, J.M.; Coutinho, F.H.; Merino, E.; Regitano, L.C.A.; Silveira, C.B.; Afli, H.; López-Pérez, M.; Rodríguez, J.C. Nasopharyngeal microbial communities of patients infected with SARS-CoV-2 that developed COVID-19. *Front. Microbiol.*, **2021**, *12*, 637430.  
<http://dx.doi.org/10.3389/fmicb.2021.637430> PMID: 33815323
- [47] Ferreira, C.; Viana, S.D.; Reis, F. Gut Microbiota dysbiosis-immune hyperresponse-inflammation triad in coronavirus disease 2019 (COVID-19): Impact of pharmacological and nutraceutical approaches. *Microorganisms*, **2020**, *8*(10), 1514.  
<http://dx.doi.org/10.3390/microorganisms8101514> PMID: 33019592
- [48] de Oliveira, G.L.V.; Oliveira, C.N.S.; Pinzan, C.F.; de Salis, L.V.V.; Cardoso, C.R.B. Microbiota modulation of the gut-lung axis in COVID-19. *Front. Immunol.*, **2021**, *12*, 635471.  
<http://dx.doi.org/10.3389/fimmu.2021.635471> PMID: 33717181
- [49] Di Stadio, A.; Costantini, C.; Renga, G.; Pariano, M.; Ricci, G.; Romani, L. The microbiota/host immune system interaction in the nose to protect from COVID-19. *Life (Basel)*, **2020**, *10*(12), 345.  
<http://dx.doi.org/10.3390/life10120345> PMID: 33322584
- [50] Sundararaman, A.; Ray, M.; Ravindra, P.V.; Halami, P.M. Role of probiotics to combat viral infections with emphasis on COVID-19. *Appl. Microbiol. Biotechnol.*, **2020**, *104*(19), 8089-8104.  
<http://dx.doi.org/10.1007/s00253-020-10832-4> PMID: 32813065
- [51] Mumford, H.; Docx, C.J.; Price, M.E.; Green, A.C.; Tattersall, J.E.; Armstrong, S.J. Human plasma-derived BuChE as a stoichiometric bioscavenger for treatment of nerve agent poisoning. *Chem. Biol. Interact.*, **2013**, *203*(1), 160-166.  
<http://dx.doi.org/10.1016/j.cbi.2012.08.018> PMID: 22981459
- [52] Wu, Y.; Zhangsun, D.; Zhu, X.; Kaas, Q.; Zhangsun, M.; Harvey, P.J.; Craik, D.J.; McIntosh, J.M.; Luo, S.  $\alpha$ -Conotoxin [S9A]TxID potently discriminates between  $\alpha 3\beta 4$  and  $\alpha 6/\alpha 3\beta 4$  nicotinic acetylcholine receptors. *J. Med. Chem.*, **2017**, *60*(13), 5826-5833.  
<http://dx.doi.org/10.1021/acs.jmedchem.7b00546> PMID: 28603989
- [53] Albulescu, L.O.; Kazandjian, T.; Slagboom, J.; Bruyneel, B.; Ainsworth, S.; Alsolaiss, J.; Wagstaff, S.C.; Whiteley, G.; Harrison, R.A.; Ulens, C.; Kool, J.; Casewell, N.R. A Decoy-receptor approach using nicotinic acetylcholine receptor mimics reveals their potential as novel therapeutics against neurotoxic snakebite. *Front. Pharmacol.*, **2019**, *10*, 848.

- http://dx.doi.org/10.3389/fphar.2019.00848 PMID: 31417406
- [54] Chen, H.Y.; Wang, W.W.; Chaou, C.H.; Lin, C.C. Prognostic value of serial serum cholinesterase activities in organophosphate poisoned patients. *J. Emerg. Med.*, **2009**, *27*(9), 1034-1039. <http://dx.doi.org/10.1016/j.ajem.2008.07.006> PMID: 19931747
- [55] Nakajima, K.; Abe, T.; Saji, R.; Ogawa, F.; Taniguchi, H.; Yamaguchi, K.; Sakai, K.; Nakagawa, T.; Matsumura, R.; Oi, Y.; Nishii, M.; Takeuchi, I. Serum cholinesterase associated with COVID-19 pneumonia severity and mortality. *J. Infect.*, **2021**, *82*(2), 282-327. <http://dx.doi.org/10.1016/j.jinf.2020.08.021> PMID: 32822684
- [56] Courties, A.; Boussier, J.; Hadjadj, J.; Yatim, N.; Barnabei, L.; Péré, H.; Veyer, D.; Kernéis, S.; Carlier, N.; Pène, F.; Rieux-Laucat, F.; Charbit, B.; Bondet, V.; Duffy, D.; Berenbaum, F.; Terrier, B.; Sellam, J. Regulation of the acetylcholine/ $\alpha$ 7nAChR anti-inflammatory pathway in COVID-19 patients. *Sci. Rep.*, **2021**, *11*(1), 11886. <http://dx.doi.org/10.1038/s41598-021-91417-7> PMID: 34088975



## Supplementary Material

### Could Small Neurotoxins-Peptides be Expressed during SARS-CoV-2 Infection?

Concetta Cafiero<sup>1,\*</sup>, Alessandra Micera<sup>2,\*</sup>, Agnese Re<sup>3</sup>, Loredana Postiglione<sup>4</sup>, Andrea Cacciamani<sup>2</sup>, Beniamino Schiavone<sup>5</sup>, Giulio Benincasa<sup>6</sup> and Raffaele Palmirotta<sup>7</sup>

<sup>1</sup>Medical Oncology, SG Moscati Hospital, Taranto, Italy; <sup>2</sup>Research Laboratories in Ophthalmology, IRCCS - Fondazione Bietti, Rome, Italy; <sup>3</sup>Department of Chemistry and Clinical Biochemistry, Catholic University of Sacred Heart, Fondazione Policlinico Universitario Agostino Gemelli IRCCS, Rome, Italy; <sup>4</sup>Department of Translational Medical Sciences, University of Federico II, Naples, Italy; <sup>5</sup>General Management Unit, Pineta Grande Hospital, Castel Volturno (CE), Italy; <sup>6</sup>Department of Clinical Pathology and Molecular Biology, Pineta Grande Hospital, Castel Volturno, (CE), Italy; <sup>7</sup>Interdisciplinary Department of Medicine, University of Bari 'Aldo Moro', School of Medicine, Italy

**Supplementary Table 1.** Protein Sequence Alignment performed using EMBOSS Needle between SARS-CoV-2 spike glycoprotein (GenBank: NC\_045512.2) and several conotoxins protein. Black: spike structural protein. Blue: Conotoxin proteins. Red: SARS-COV-2 RBD epitope sequence for the CR3022 mAb. Framework: highly conserved region of SARS-CoVs RBD (aa 375–395). (|): identities, (:) conservative replacements, (.) non-conservative replacements.

Protein Sequence Alignment between SARS-CoV-2 spike glycoprotein (GenBank: NC\_045512.2) and Neurotoxin homolog NL1, *Naja atra* (Chinese cobra) (UniProtKB - Q9DEQ3 - 3SO8\_NAJAT)\* protein [ref. Farsalinos et al. 2020c].

\*This sequence is similar to Muscarinic toxin-like protein, *Bungarus multicinctus* (Many-banded krait) (UniProtKB: Q9W727 - 3SO8\_BUNMU)

**MKTL L L T L V V V T M V C M D L G Y T T I C Y N H L S R T P E T T E I C P D S W Y F C Y K I S - L A D G N D V R I K R G C T F T C P E L R P T G K Y V Y C C R R D K C N Q**

EMBOSS_001	1	MFVFLVLLPLVSSQCVNLTTRTQLPPAYTNSFTRGVYYPDKVFRSSVLHS	50
EMBOSS_001	51	TQDLFLPFFSNVTWFHAIHVSGTNGTKRFDNPVLPFNDGVYFASTEKSN	100
EMBOSS_001	101	IRGWIFGTTLDSTQSLIVNNAATNVVIKVCFEQFCNDPFLGVYHKNK	150
EMBOSS_001	151	SWMESEFRVYSSANNCTFEYVSQPFLMDLEGKQGNFKNLREFVFKNIDGY	200
EMBOSS_001	201	FKIYSKHTPINLVRDLPQGFSALEPLVDLPIGINITRFQTLALHRSYLT	250
EMBOSS_001	1	-----MKTL L L T L-----AVVTMV-CMDLGYT-TI	23
EMBOSS_001	251	PGDSSSGWTAGAAAYVGYLQPRTFLLKYNENGTITDAVDCALDPLSETK	300
EMBOSS_001	24	C-----Y-----NHL S R T P E T T E I C P D S W Y F C --YKISL	50
EMBOSS_001	301	CTLKSF TVEKGIYQTSNFRVQPTESIVRFPNITNLCPFGEVFNATRFASV	350
EMBOSS_001	51	ADGNDVRIKRG C-----TFTCP EL R P T G K Y V Y C C-----	79
EMBOSS_001	351	YAWNRRKRIS-NCVADYSVL YNSA FSTFKCYGVSPT-KLNDLCFTNVYAD	398



EMBOSS_001	80	-----RRDKCNQ-----	86
		.: :..	
EMBOSS_001	399	SFVIRGDEVQRQIAPGQTGKIADYNYKLPDDFTGCVIAWNSNNLDSKVGGN	448
EMBOSS_001	449	YNYLYRLFRKSNLKPFERDISTEIQAGSTPCNGVEGFNCYFPLQSYGFQ	498
EMBOSS_001	499	PTNGVGYQPYPYRVVLSFELLHAPATVCGPKKSTNLVKNKCVNFNENGLTG	548
EMBOSS_001	549	TGVLTESNKKFLPFQQFGRDIADTTDAVRDPQTLEILDITPCSFGGVSVI	598
EMBOSS_001	599	TPGTNTSNQVAVLYQDVNCTEVPVAIHADQLTPTWRVYSTGSNVFQTRAG	648
EMBOSS_001	649	CLIGAEHVNNSYECDIPIGAGICASYQTQTNSPRRARSVASQSIIAYTMS	698
EMBOSS_001	699	LGAENSVAYSNNNSIAIPTNFTISVTEILPVSMTKTSVDC TMYICGDSTE	748
EMBOSS_001	749	CSNLLLQYGSFCTQLNRALTGIAVEQDKNTQEVFAQVKQIYKTPPIKDFG	798
EMBOSS_001	799	GFNFSQILPDPSKPSKRSFIEDLLFNKVTLADAGFIKQYGDCLGDIAARD	848
EMBOSS_001	849	LICAQKFNGLTVLPPLLTDEMIAQYTSALLAGTITSGWTFGAGAAIQIPF	898
EMBOSS_001	899	AMQMAYRFNGIGVTQNVLYENQKLIANQFNSAIGKIQDSLSTASALGKL	948
EMBOSS_001	949	QDVVNQNAQALNTLVKQLSSNFGAISSVLNDILSRLDKVEAEVQIDRLIT	998
EMBOSS_001	999	GRLQSLQTYVTQQLIRAAEIRASANLAATKMSECVLGQSKRVDFCGKGYH	1048
EMBOSS_001	1049	LMSFPQSAPHGVVFLHVTVYVPAQEKNF T TAPAICHGKAHFPREGVFVSN	1098
EMBOSS_001	1099	GTHWFVTQRNFYEPQIITTDNTFVSGNCDVVIGIVNNTVYDPLQPELDSF	1148
EMBOSS_001	1149	KEELDKYFKNHTSPDVDLGDISGINASVVNIQKEIDRLNEVAKNLNESLI	1198
EMBOSS_001	1199	DLQELGKYEQYIKWPWYIWLGFIAGLIAIVMVTIMLCCMTSCC SCLKGCC	1248
EMBOSS_001	1249	SCGSCCKFDEDDSEPVLKGVKLHYT 1273	

Protein Sequence Alignment between SARS-CoV-2 spike glycoprotein (GenBank: NC\_045512.2) and **Kappa-conotoxin-like as14a**, *Conus cancellatus* (*Cancellate cone*) (*Conus austini*) (UniProtKB: P0C6S2 - CLEA\_CONCF) protein.

GGVGRCIYNCMNSGGGLNFIQCKTMCY

EMBOSS_001	1	MFVFLVLLPLVSSQCVNLTTRTQLPPAYTNSFTRGVYYPDKVFRSSVLHS	50
EMBOSS_001	51	TQDLFLPFFSNVTWFHAIHVS GTNGTKRFDNPVLPFNDGVYFASTEKSNI	100
EMBOSS_001	101	IRGWIFGTTLDSKTQSL L I V N N A T N V V I K V C E F Q C N D P F L G V Y Y H K N N K	150
EMBOSS_001	151	SWMESEFRVYSSANNCTFEYVSQPFLMDLE GKQGNFKNLREFVFKNIDGY	200
EMBOSS_001	201	FKIYSKHTPINLVRDL PQGFSALEPLVDLP IGINITRFQ TLLALHRSYLT	250
EMBOSS_001	251	PGDSSSGWTAGAAAYVGYLQPR T F L L K Y N E N G T I T D A V D C A L D P L S E T K	300
EMBOSS_001	301	CTLKSFTVEKGIYQTSNFRVQP TESIVRFPNITNLCPFGEVFNATRFASV	350
EMBOSS_001	1	-----GGVGRCI--YNCMNSGGGLNFIQC-----K T M C Y-----	27
		..... :  :.....:..:  ..: :	
EMBOSS_001	351	YAWNRKRISNCVADYSVL YNSA S F S T F K C Y G V S P T K L N D L C F T N V Y A D S F	400

EMBOSS_001	401	VIRGDEVQRQIAPGQTGKIADYNYKLPDDEF	GCVIAWNSNNLDSKVGGNYN	450
EMBOSS_001	451	YLYRFLFRKSNLKPFFERDISTEIQAGSTPCNGVEGFNCYFPLQSYGFQPT		500
EMBOSS_001	501	NGVGYQPYRVVLSFELLHAPATVCGPKKSTNLVKNKCVNFNFLTGTG		550
EMBOSS_001	551	VLTESNKKFLPFQQFGRDIADTTDAVRDPQTLLEILDITPCSFGGVSVITP		600
EMBOSS_001	601	GTNTSNQVAVLYQDVNCTEVPVAIHADQLTPTWRVYSTGSNVFQTRAGCL		650
EMBOSS_001	651	IGAEHVNSYECIDIPIGAGICASYQTQTNSPRRARSVASQSIAYTMSLG		700
EMBOSS_001	701	AENSVAYSNNNSIAIPTNFTISVTTEILPVSMKTSTVDCMYICGDSTEC		750
EMBOSS_001	751	NLLQYGSFCTQLNRALTGIAVEQDKNTQEVFAQVKQIYKTPPIKDFGGF		800
EMBOSS_001	801	NFSQILPDPSPKRSFIEDLLFNKVTLLADAGFIKQYGDCLGDI AARDLI		850
EMBOSS_001	851	CAQKFNGLTVLPLLLTDEMIAQYTSALLAGTITSGWTFGAGAALQIPFAM		900
EMBOSS_001	901	QMAYRFNGIGVTVQNVLYENQKLIANQFNSAIGKIQDSLSTASALGKLQD		950
EMBOSS_001	951	VVNQAQALNTLVKQLSSNFGAISSVLNDILSRDKVEAEVQIDRLITGR		1000
EMBOSS_001	1001	LQSLQTYVTQQLIRAAEIRASANLAATKMSECVLGQSKRVDFCGKGYHLM		1050
EMBOSS_001	1051	SFPQSAPHGVVFLHVTYVPAQEKNTTAPAICHGKAHFPREGVFSNGT		1100
EMBOSS_001	1101	HWFVTQRNFYEQIITTDNTFVSGNCDVVIGIVNNTVYDPLQPELDSFKE		1150
EMBOSS_001	1151	ELDKYFKNHTSPDVLGDISGINASVVNIQKEIDRLNEVAKNLNESLIDL		1200
EMBOSS_001	1201	QELGKYEQYIKWPWYIWLGFIAGLIAIVMVTIMLCCMTSCCSCLKGCCSC		1250
EMBOSS_001	1251	GSCCKFDEDDSEPVKGVKLHYT	1273	

Protein Sequence Alignment between SARS-CoV-2 spike glycoprotein (GenBank: NC\_045512.2) and Rho-conotoxin TIA (CA1A\_CONTU), Conus tulipa (Fish-hunting cone snail) (Tulip cone) (UniProtKB: P58811) protein.

MFTVFLVVLATTGVSFTLDRASDGGNAVAKKSDVTARFNWRCCLIPACRRNHKKFCG

EMBOSS_001	1	MFVFLVLLPLVSSQCVNLTTRTQLPPAYTNSFTRGVYYPDKVFRSSVLHS		50
EMBOSS_001	51	TQDLFLPFFSNVTWFHAIHVSNGTKRFDNPVLPFNDGVYFASTEKSNI		100
EMBOSS_001	101	IRGWIFGTTLDSKTQSLIVNNAATNVVIVKVFQFCNDPFLGVYHKNK		150
EMBOSS_001	151	SWMESEFRVYSSANNCTFEYVSQPFLMDLEGKQGNFKNLREFVFNIDGY		200
EMBOSS_001	201	FKIYSKHTPINLVRDLPQGFSALEPLVDLPIGINITRFQTLALHRSYLT		250
EMBOSS_001	251	PGDSSSGWTAGAAAYVGYLQPRTFLLKYNENGTITDAVDCALDPLSETK		300
EMBOSS_001	301	CTLKSFTVEKGIYQTSNFRVQPTESIVRFPNITNLCPFGEVFNATRFASV		350
EMBOSS_001	351	YAWNKRKISNCVADYSVL <del>YNSASFSTFKCYGVSPTKLNDL</del> CFTNVYADSF		400
EMBOSS_001	401	VIRGDEVQRQIAPGQTGKIADYNYKLPDDEF	GCVIAWNSNNLDSKVGGNYN	450
EMBOSS_001	451	YLYRFLFRKSNLKPFFERDISTEIQAGSTPCNGVEGFNCYFPLQSYGFQPT		500
EMBOSS_001	501	NGVGYQPYRVVLSFELLHAPATVCGPKKSTNLVKNKCVNFNFLTGTG		550



EMBOSS_001	651	IGAEHVNNSEYECDIPIGAGICASYQTQTNSPRRARSVASQSIIAYTMSLG	700
EMBOSS_001	701	AENSVAYSNNNSIAIPTNFTTISVTTEILPVSMTKTSVDCTMYICGDSTEC	750
EMBOSS_001	751	NLLLOYGSFCTQLNRALTGIAVEQDKNTQEVFAQVKQIYKTPPIKDFGGF	800
EMBOSS_001	801	NFSQILPDPSPKSKRSFIEDLLEFNKVTLLADAGFIKQYGDCLGDIARDLI	850
EMBOSS_001	851	CAQKFNGLTVLPPLLTDEMIAYTSALLAGTITSGWTFGAGAALQIPFAM	900
EMBOSS_001	901	QMAYRFNGIGVTONVLYENQKLIANQFNSAIGKIQDLSLSTASALGKLD	950
EMBOSS_001	951	VVNQNAQALNTLVKQLSSNFGAISSVLNDILSRLDKVEAEVQIDRLITGR	1000
EMBOSS_001	1001	LQSLQTYVTQQLIRAAEIRASANLAATKMSECVLGQSKRVDFCGKGYHLM	1050
EMBOSS_001	1051	SFPQSAPHGVVFLHVTVYVPAQEKNFTTAPAICHGKAHFPREGVFSNGT	1100
EMBOSS_001	1101	HWFVTQRNFYEQIITTDNTFVSGNCDVVIGIVNNTVYDPLQPELDSFKE	1150
EMBOSS_001	1151	ELDKYFKNHTSPDVLGDISGINASVVNIQKEIDRLNEVAKNLNESLIDL	1200
EMBOSS_001	1	-----MGMRRMFTVFLLVLLATTVVSTPSDRASDGRNA	33
		:   ... :~::~~::~	
EMBOSS_001	1201	QELGKYEQYIKWPWYIWLG---FIAGLIAIVMVTIML-----	1234
EMBOSS_001	34	AVHERQKSLVPSVITTCGGYDPGTMCPPCRCTNSCG-----	69
		..: : ...     . . . .	
EMBOSS_001	1235	-----CCMTSCCCLKG--C--CSCGSCCKFDEDDSEPVKGVK	1269
EMBOSS_001	1270	LHYT 1273	

Protein Sequence Alignment between SARS-CoV-2 spike glycoprotein (GenBank: NC\_045512.2) and Conotoxin C114.9, *Californiconus californicus* (*California cone*) (*Conus californicus*) (UniProtKB: D6C4J8 - CUE9\_CONCL) protein.

MTAKATLLVLALVVMATSGVSSASVAGGPVVNSDITVSRSDPERLSTRGCVANCQANQTGIDCIKYCGIGIGRRDITQQ

EMBOSS_001	1	MFVFLVLLPLVSSQCVNLTTRTQLPPAYTNSFTRGVYYPDKVFRSSVLHS	50
EMBOSS_001	51	TQDLFLPFFSNVTWFHAIHVSNGTKRFDNPVLPFNDGVYFASTEKSNI	100
EMBOSS_001	101	IRGWIFGTTLDSKTQSLLIIVNNATNVVIKVFQFCNDPFLGVYHKNK	150
EMBOSS_001	151	SWMESEFRVYSSANNCTFEYVSQPFLMDLEGKQGNFKNLREFVFNIDGY	200
EMBOSS_001	201	FKIYSKHTPINLVRDLPOGFSALEPLVDLPIGINITRFQTLALHRSYLT	250
EMBOSS_001	251	PGDSSSGWTAGAAAYVGYLQPRTFLLKYNENGTITDAVDCALDPLSETK	300
EMBOSS_001	301	CTLKSFTVEKGIYQTSNFRVQPTESIVRFPNITNLCPFGEVFNATRFASV	350
EMBOSS_001	351	YAWNRKRISNCVADYSVL <b>YNSAS</b> <span style="border: 1px solid black; padding: 2px;">STFKCYGVSPTKLNDL</span> CFTNVYADSF	400
EMBOSS_001	401	VIRGDEVQRQIAPGQTGKIADYNYKLPDDEF <b>T</b> GCVIAWNSNNLDSKVGNYN	450
EMBOSS_001	451	YLYRFLFRKSNLKPFFERDISTEYIYQAGSTPCNGVEGFNCYFPLQSYGFQPT	500
EMBOSS_001	501	NGVGYQPYRVVLS <b>FELL</b> HAPATVCGPKKSTNLVKNKCVNFENGLTGTG	550
EMBOSS_001	551	VLTESNKKFLPFQOQFRDIADTTDAVRDPQTEILDITPCSFGGVSVITP	600
EMBOSS_001	601	GTNTSNQVAVLYQDVNCTEVPVAIHADQLTPTWRVYSTGSNVFQTRAGCL	650

EMBOSS_001	1	-----MTAKATLLVLAIVVM	15
		.. .....	
EMBOSS_001	651	IGAHEVNNSECDIPIGAGICASYQTQTNsprrarsvasqsIIAYTMSLG	700
EMBOSS_001	16	ATSGV--SSASVAGGPVNSDTSRSDPERLSTRGCVANCQANQTGIDCI	63
		.:.   .:.   .:.: :  :.:  . :.....: : .	
EMBOSS_001	701	AENSVAYSNNSIA---IPTNFTIS-----VTTE--ILPVSMTKTSDVCT	739
EMBOSS_001	64	KY-CGIGIGRRDITQQ-----	78
		.      .:.	
EMBOSS_001	740	MYICG-----DSTECSNLLLQYGSFCTQLNRALTGIAVEQDKNTQEVFA	783
EMBOSS_001	784	QVKQIYKTPPIKDFGGFNFSQILPDPSKPSKRSFIEDLLFNKVTLDAGF	833
EMBOSS_001	834	IKQYGDCLGDIAARDLICAQKFNGLTVLPPLLTDEMIAQYTSALLAGTIT	883
EMBOSS_001	884	SGWTFGAGAALQIPFAMQMAYRFNGIGVTQNVLYENQKLIANQFNSAIGK	933
EMBOSS_001	934	IQDSLSTASALGKLQDVVNQNAQALNTLVKQLSSNFGAISSVLDILSR	983
EMBOSS_001	984	LDKVEAEVQIDRLITGRLQSLQTYVTQQLIRAAEIRASANLAATKMSECV	1033
EMBOSS_001	1034	LGQSKRVDFCGKGYHLSMFPQSAPHGVVFLHVTVVPAQEKNETTAPAICH	1083
EMBOSS_001	1084	DGKAHFPPREGVFSVNGTHWFVTQRNFYEPQIITDNTFVSGNCDVVIGIV	1133
EMBOSS_001	1134	NNTVYDPLQPELDSFKEELDKYFKNHTSPDVLGDISGINASVVNIQKEI	1183
EMBOSS_001	1184	DRLNEVAKNLNESLIDLQELGKYEQYIKWPWYIWLGFIAGLIAIVMVTIM	1233
EMBOSS_001	1234	LCCMTSCCSCLKGCCSCGCKFDEDDSEPVKGVKLHYT 1273	

Protein Sequence Alignment between SARS-CoV-2 spike glycoprotein (GenBank: NC\_045512.2) and Alpha-conotoxin SII, *Conus striatus* (*Striated cone*) (UniProtKB: P28879- CAS2\_CONST) protein.

MGMRMMFTVFLVVLATTVVSFSDRASDGRDDEAKDERSDMHESDRNGRGCNCPACGPNYGCSTCSRTL

EMBOSS_001	1	MEVFLVLLPLVSSQCVNLTTRTQLPPAYTNSFTRGVYYPDKVFRSSVLHS	50
EMBOSS_001	51	TQDLFLPFFSNVTWFHAIHVSNGTNGTKRFDNPVLPFNDGVYFASTEKSNI	100
EMBOSS_001	101	IRGWIFGTTLDSTQSLIVNATNVVIKVFCEQFCNDPFLGVYHKNK	150
EMBOSS_001	151	SWMESEFRVYSSANNCTFEYVSQPFMDLEKQGNFKNLREVFVKNIDGY	200
EMBOSS_001	201	FKIYSKHTPINLVRDLPGFSALEPLVDLPIGINITRFQTLALHRSYLT	250
EMBOSS_001	251	PGDSSSGWTAGAAAYVGYLQPRTFLLKYNENGTITDAVDCALDPLSETK	300
EMBOSS_001	301	CTLKSFTVEKGIYQTSNFRVQPTESIVRFPNITNLCPFGEVFNATRFASV	350
EMBOSS_001	351	YAWNRKRISNCVADYSVL <b>YNSAS</b> <span style="border: 1px solid black; padding: 2px;">STFKCYGVSPTKLN</span> <b>DL</b> CFITNVYADSF	400
EMBOSS_001	401	VIRGDEVQRQIAPGQTGKIADYNYKLPDDEFTGCVIAWNSNLDKSVGGNYN	450
EMBOSS_001	451	YLYRFLFRKSNLKPFFERDISTEIQAGSTPCNGVEGFNCYFPLQSYGFQPT	500
EMBOSS_001	501	NGVGYQPYRVVLS <b>FELL</b> HAPATVCGPKKSTNLVKNKCVNFNFLGTGTG	550
EMBOSS_001	551	VLTESNKKFLPFQFGRDIADTTDAVRDPQTLIELDITPCSFGGVSVITP	600
EMBOSS_001	601	GTNTSNQVAVLYQDVNCTEVPVAIHADQLTPFWRVYSTGNSVVFQTRAGCL	650
EMBOSS_001	651	IGAHEVNNSECDIPIGAGICASYQTQTNsprrarsvasqsIIAYTMSLG	700
EMBOSS_001	701	AENSVAYSNNSIAIPTNFTISVTTEILPVSMTKTSDVCTMYICGDSTECS	750

EMBOSS_001	751	NLLLOYGSFCTQLNRALTGIAVEQDKNTQEVFAQVKQIYKTPPIKDFGGF	800
EMBOSS_001	801	NFSQILPDPSKPSKRSFIEDLLFNKVTLLADAGFIKQYGDCLGDI AARDLI	850
EMBOSS_001	851	CAQKFNGLTVLPPLLTDEMI AQYTSALLAGTITSGWTFGAGAALQIPFAM	900
EMBOSS_001	901	QMAYRFNGIGVTONVLYENQKLIANQFN SAIGKIQDSLSTASALGKLQD	950
EMBOSS_001	951	VVNQNAQALN TLVKQLSSNFGAISSVLNDILSRLDKVEAEVQIDRLITGR	1000
EMBOSS_001	1001	LQSLQTYVTQQLIRAAEIRASANLAATKMSECVLGQSKRVDFCGKGYHLM	1050
EMBOSS_001	1051	SFPQSAPHGVVFLHVTVVPAQEKNFTTAPAICH DGKAHFPREGVFVSNGT	1100
EMBOSS_001	1101	HWFVTQRNFYEQIITTDNTFVSGNCDVVIGIVNNTVYDPLQPELDSFKE	1150
EMBOSS_001	1151	ELDKYFKNHTSPVDLGDISGINASVVNIQKEIDRLNEVAKNLNESLIDL	1200
EMBOSS_001	1	-----MGMRMMFTVFLLVVLATTVVSFPSDRASDGRDD	33
		:   ... :~::~ :~:	
EMBOSS_001	1201	QELGKYEQYIKWPWYIWLG----FIAGLIAIVMVTIML-----	1234
EMBOSS_001	34	EAKDERSDMHESDRNDRGCCNPACGPNYCGCTSCSRTL-----	72
		... ...   .  ...:	
EMBOSS_001	1235	-----CCMTSCCCLKGC-CSCGSCCKFDEDDSEPVL	1265
EMBOSS_001	1266	KGVKLHYT 1273	

Protein Sequence Alignment between SARS-CoV-2 spike glycoprotein (GenBank: NC\_045512.2) and Conotoxin 10, *Conus virgo* (*Virgin cone*) (UniProtKB: Q5K0C5 - O16A\_CONVR) protein.

MKLTCVLITVFLTLTASQLITADYSRDQRQYRAVRLGDEMRFKRGARDCGGQEGCYTQPCCPGLRCRGGGTGGGACQL

EMBOSS_001	1	MFVFLVLLPLVSSQCVNLTTRTQLPPAYTNSFTRGVYYPDKVFRSSVLHS	50
EMBOSS_001	51	TQDLFLPFFSNVTWFHAIHVS GTNGTKRFDNPVLPFNDGVYFASTEKSNI	100
EMBOSS_001	101	IRGWIFGTTLDSKTQSL LIVN NATNVVIKVECFQCNDPFLGVYYHKNNK	150
EMBOSS_001	151	SWMESEFRVYSSANNCTFEYVSQPFLMDLEGKQGNFKNLREFVFKNIDGY	200
EMBOSS_001	201	FKIYSKHTPINLVRDLPQGFSALEPLVDLPIGINITRFQTL LALHRSYLT	250
EMBOSS_001	251	PGDSSSGWTAGAAAYVGYLQRTFLLKYNENGTITDAVDCALDPLSETK	300
EMBOSS_001	301	CTLKSFTVEKGIYQTSNFRVQPTESIVRFPNITNLCPFGEVFNATRFASV	350
EMBOSS_001	351	YAWNKRKISNCVADYSVL YNSAS <b>STFKCYGVSPTKLN DL</b> CFTNVYADSF	400
EMBOSS_001	401	VIRGDEV RQIAPGQTGKIADYNYKLP <b>DDFT</b> GCVIAWNSNNLDSKVGGNYN	450
EMBOSS_001	451	YLYR LFRKSNLKPFERDISTEIYQAGSTPCNGVEGFNCYFPLQSYGFQPT	500
EMBOSS_001	501	NGVGYQPYRVVLS <b>FELLH</b> APATVCGPKKSTNLVKNKCVNFENGLTGTG	550
EMBOSS_001	551	VLTESNKKFLPFQQFGRDIADTTDAVRDPQ TLEILDITPCSFGGVSVITP	600
EMBOSS_001	601	GTNTSNQVAVLYQDVNCTEVPVAIHADQLTPTWRVYSTG SNVFQTRAGCL	650
EMBOSS_001	651	IGA EHVNNSYECDIPIGAGICASYQTQTNSPRRARSVASQSI IAYTMSLG	700
EMBOSS_001	701	AENSVAYSNN SIAIPTNFTISVTTEILPVSMTKTSVDC TMYICGDSTEC S	750

EMBOSS_001	751	NLLLQYGSFCTQLNRALTGIAVEQDKNTQEVFAQVKQIYKTPPIKDFGGF	800
EMBOSS_001	801	NFSQILPDPSPKRSFIEDLLFNKVTLADAGFIKQYGDCLGDIARDLI	850
EMBOSS_001	851	CAQKFNGLTVLPPLLTDEMIQYTSALLAGTITSGWTFGAGAALQIPFAM	900
EMBOSS_001	901	QMAYRFNGIGVTVQNVLYENQKLIANQFNNSAIGKIQDSLSTASALGKLQD	950
EMBOSS_001	951	VVNQNAQALNTLVKQLSSNFGAISSVLNDILSRLDKVEAEVQIDRLITGR	1000
EMBOSS_001	1001	LQSLQTYVTQQQLIRAAEIRASANLAATKMSECVLGQSKRVDFCGKGYHLM	1050
EMBOSS_001	1051	SFPQSAPHGVVFLHVTVYVPAQEKNFHTTAPAICHDKGAHFPREGVVFVSNGT	1100
EMBOSS_001	1101	HWFVTQRNFYEQIITTDNTFVSGNCDVVIGIVNNTVYDPLQPELDSFKE	1150
EMBOSS_001	1151	ELDKYFKNHTSPDVLGDISGINASVVNIQKEIDRLNEVAKNLNESLIDL	1200
EMBOSS_001	1	-----MKLTCVLIITVFLFTASQLITADYSRDQR	29
		.. ...::: :..	
EMBOSS_001	1201	QELGKYEQYIKWPWYIWLGFIAGLIAIVMVTIML-----	1234
EMBOSS_001	30	QYRAVRLGDEMRFKRGARDCGGQEGECYTQPCCPGLRCRGGGTGGGACQL	79
		...  ..  : ... .. :..	
EMBOSS_001	1235	-----CCMTSCCSCL--KGCCSCGSCCKF	1256
EMBOSS_001	1257	DEDDSEPVLKGVKLHYT	1273

Protein Sequence Alignment between SARS-CoV-2 spike glycoprotein (GenBank: NC\_045512.2) and Alpha-conotoxin-like Pu1.5, Alpha-conotoxin-like Pu1.5 (UniProtKB: P0C8U9 - CA15\_CONPL) protein.

MFTVFLLVILATTVVFPSPDRDPASNHENSKGSNRNAWLTPEECCAAPACREMILEFCLAGEAFAAALDGFRRLPYRLSSE

EMBOSS_001	1	MFVFLVLLPLVSSQCVNLTTRTQLPPAYTNSFTRGVYYPDKVFRSSVLHS	50
EMBOSS_001	51	TQDLFLPFFSNVTWFHAIHVSGTNGTKRFDNPVLPFNDGVYFASTEKSNI	100
EMBOSS_001	1	-----MFTVFLLVILATTVV----FPSPDRDP----ASNHENSK	31
		..... : ..   ..  . .....   ... : :	
EMBOSS_001	101	IRGWIFGTTLDSKTQSLIVNNAATNVVIVKVFQFCNDPFLGVYYHKNNK	150
EMBOSS_001	32	GSNRNAWLTPE--ECCAAPACREMILEFCLAGEAFAAALDG----FRRLP	75
		: :..   ... ..  . .....: ... :   :..	
EMBOSS_001	151	-----SWMESEFRVYSSANNC-----TFEYVSQPFLMDLEGKQGNFKNLR	190
EMBOSS_001	76	-----YRLSSE-----	81
		::: :	
EMBOSS_001	191	EFVFKNIDGYFKIYKHTPINLVRDLPQGFSALEPLVDLPIGINITRFQT	240
EMBOSS_001	241	LLALHRSYLTPGDSSSGWTAGAAAYVGYLQPRTFLLKYNENGTITDAVD	290
EMBOSS_001	291	CALDPLSETKCTLKSFTVEKGIYQTSNFRVQPTESIVRFPNITNLCPFGE	340
EMBOSS_001	341	VFNATRFASVYAWNKRKISNCVADYSVL <del>YNSASF</del> <b>STFKCYGVSPTKLNLDI</b>	390
EMBOSS_001	391	CFTNVYADSFVIRGDEVQRQIAPGQTGKIADYNYKLP <b>DDFT</b> GCVIAWNSNN	440
EMBOSS_001	441	LDSKVGNYNYLYRLFRRKSNLKPFFERDISTEIYQAGSTPCNGVEGFNCYF	490
EMBOSS_001	491	PLQSYGFQPTNGVGYQPYRVVLS <b>FELL</b> HAPATVCGPKKSTNLVKNKCVN	540
EMBOSS_001	541	FNFNGLTGTGVLTESNKKFLPFQGFGRDIADTTDAVRDPQTLIILDITPC	590
EMBOSS_001	591	SFGGVSVITPGTNTSNQVAVLYQDVNCTEVPVAIHADQLTPTWRVYSTGS	640
EMBOSS_001	641	NVFQTRAGCLIGAEHVNNSECDIPIGAGICASYQTQTNSPRRARVASQ	690





EMBOSS_001	699	LGAENSVAYSNNNSIAIPTNFTISVTTTEILPVSMTKTSVDCTMYICGDSTE	748
EMBOSS_001	749	CSNLLLQYGSFCTQLNRALTGIAVEQDKNTQEVFAQVKQIYKTPPIKDFG	798
EMBOSS_001	799	GFNFSQILPDPSPKSKRSFIEDLLFNKVTLADAGFIKQYGDCLGDIAARD	848
EMBOSS_001	849	LICAQKFNGLTVLPPLLTDEMIQYTSALLAGTITSGWTFGAGAALQIPF	898
EMBOSS_001	899	AMQMAYRFNGIGVTVQNVLYENQKLIANQFNSAIGKIQDLSSTASALGKL	948
EMBOSS_001	949	QDVVNQNAQALNTLVKQLSSNFGAISSVLNDILSRLDKVEAEVQIDRLIT	998
EMBOSS_001	999	GRLQSLQTYVTQQLIRAAEIRASANLAATKMSECVLGQSKRVDFCGKGYH	1048
EMBOSS_001	1049	LMSFPQSAPHGVVFLHVTVYVPAQEKNFHTTAPAICHDKGAHFPREGVFSN	1098
EMBOSS_001	1099	GTHWFVTQRNFYEQIITTDNTFVSGNCDVVIGIVNNTVYDPLQPELDSF	1148
EMBOSS_001	1149	KEELDKYFKNHTSPDVLGDISGINASVVNIQKEIDRLNEVAKNLNESLI	1198
EMBOSS_001	1199	DLQELGKYEQYIKWPWYIWLGFIAGLIAIVMVTIMLCCMTSCCCLKGCC	1248
EMBOSS_001	1249	SCGSCCKFDEDDSEPVLKGVKLHYT 1273	

Protein Sequence Alignment between SARS-CoV-2 spike glycoprotein (GenBank: NC\_045512.2) and Conotoxin C19.6, *Californiconus californicus* (*California cone*) (*Conus californicus*) (UniProtKB: D6C4M3 - CU96\_CONCL) protein.

MSTLGMTLLLLLLPLATPDDVGQPPKRDTLRNLKIGTRGQGGCVPPGGGRCKANQACTKGGNPGTCGFQYDLCLCLRN

EMBOSS_001	1	MSTLGMTLLLLLLPLATPDDVGQPPKRDTLRNLKIGTRGQGGCVPPG	50
EMBOSS_001	1	-----MFVFLVLLPLVSSQCV-----NLTRTRQ---LPP-	26
EMBOSS_001	51	GGRCKANQACTKGGNPGTCGFQY-----DLCLCLRN-----	81
EMBOSS_001	27	-----AYT---NSFTRGVYYPDKVFRSSVLHSTQDLFLPFFSNVTWF	65
EMBOSS_001	66	HAIHVSGTNGTKRFDNPVLPFNDGVYFASTEKSNIIRGWIFGTTLDSKTQ	115
EMBOSS_001	116	SLLIVNNA TNVVIKVECFQCNDPFLGVYYHKNNKSWMESEFRVYSSANN	165
EMBOSS_001	166	CTFEYVSQPFLMDLEGGKQGNFKNLREFVFKNIDGYFKIYSKHTPINLVRD	215
EMBOSS_001	216	LPQGFSALEPLVDLPIGINITRFQTLALHRSYLTPGDSSSGWTAGAAAY	265
EMBOSS_001	266	YVGYLQPRTFLLKYNENGTITDAVDCALDPLSETKCTLSFTVEKGIYQT	315
EMBOSS_001	316	SNFRVQPTESIVRFPNITNLCPFGEVFNATRFASVYAWNRRKRSNCVADY	365
EMBOSS_001	366	SVLYNSASFSTFKCYGVSPTKLNDL	415
EMBOSS_001	416	GKIADYNYKLPDDFTGCVIAWNSNNLDSKVGNYNYLYRLFRKSNLKPFE	465
EMBOSS_001	466	RDISTEIIYQAGSTPCNGVEGFNCYFPLQSYGFQPTNGVGYQPYRVVLSF	515
EMBOSS_001	516	ELLHAPATVCGPKKSTNLVKNKCVNFNFNGLTGTGVLTESNKKFLPFQOF	565
EMBOSS_001	566	GRDIADTTDAVRDPQTLLEILDITPCSFGGVSVITPGTNTSNQVAVLYQDV	615
EMBOSS_001	616	NCTEVPVAIHADQLTPTWRVYSTGSNVFQTRAGCLIGAEHVNSYECDIP	665
EMBOSS_001	666	IGAGICASYQTQNSPRRARSVASQSIIAYTMSLGAENSVAYSNNNSIAIP	715
EMBOSS_001	716	TNFTISVTTTEILPVSMTKTSVDCTMYICGDSTECSNLLLQYGSFCTQLNR	765

EMBOSS_001	766	ALTGIAVEQDKNTQEVFAQVKQIYKTPPIKDFGGFNFSQILPDPSPKPSKR	815
EMBOSS_001	816	SFIEDLLFNKVTLADAGFIKQYGDCLGDI AARDLICAQKFNGLTVLPPLL	865
EMBOSS_001	866	TDEMIAQYTSALLAGTITSGWTFGAGAALQIPFAMQMAYRFNGIGVTQNV	915
EMBOSS_001	916	LYENQKLIANQFN SAIGKIQDSLSTASALGKLQDVVNQNAQALNTLVKQ	965
EMBOSS_001	966	LSSNFGAISSVLNDILSRDKVEAEVQIDRLITGRLQSLQTYVVTQQLIRA	1015
EMBOSS_001	1016	AEIRASANLAATKMSECVLGQSKRVDFCGKGYHLMSFPQSAPHGVVFLHV	1065
EMBOSS_001	1066	TYVPAQEKNF T TAPAICHGKAHFPREGV FVSNGTHWFVTQRNFYEPQII	1115
EMBOSS_001	1116	TTDNTFVSGNCDVVIGIVNNTVYDPLQPELDSFKEELDKYFKNHTSPDVD	1165
EMBOSS_001	1166	LGDISGINASV VNIQKEIDRLNEVAKNLNESLIDLQELGKYEQYIKWPWY	1215
EMBOSS_001	1216	IWLGFIAGLIAIVMVTIMLCCMTSCCCLKGCSCGSCCKFDEDDSEPVL	1265
EMBOSS_001	1266	KGVKLHYT 1273	

Protein Sequence Alignment between SARS-CoV-2 spike glycoprotein (GenBank: NC\_045512.2) and Conotoxin Vi15a, *Conus virgo* (Virgin cone), (UniProtKB: B3FIA5 - CVFA\_CONVR) protein.

MMPVILLLLLSLAIRCADGKAVQGDSDPSASLLTGDKNHDLPVKRDC TTCAGEECCGRCTCPWGDNCSCIEWGK

EMBOSS_001	1	MFVFLVLLPLVSSQCVNLTTRTQ LPPAYTNSFTRGVYYPDKVFRSSVLHS	50
EMBOSS_001	51	TQDLFLPFFSNVTWFHAIHVS GTNGTKRFDNPVLPFNDGVYFASTEKSNI	100
EMBOSS_001	101	IRGWIFGTTLDSKTQSL L I V N N A T N V V I K V C E F Q C N D P F L G V Y Y H K N N K	150
EMBOSS_001	151	SWMESEFRVYSSANNCTFEYVSQPFLMDLEGKQGNFKNLREFVFKNIDGY	200
EMBOSS_001	201	FKIYSKHTPINLVRDLPQGFSALEPLVDLPIGINITRFQTL LALHRSYLT	250
EMBOSS_001	251	PGDSSSGWTAGAAAYVGYLQPR T F L L K Y N E N G T I T D A V D C A L D P L S E T K	300
EMBOSS_001	301	CTLKSFTVEKGIYQTSNFRVQPTESIVRFPNITNLCPFGEVFNATRFASV	350
EMBOSS_001	351	YAWNKRKISNCVADYSVL <b>YNSASFSTFKCYGVSPTKLN</b> DL CFTNVYADSF	400
EMBOSS_001	401	VIRGDEV R Q I A P G Q T G K I A D Y N Y K L P D D F T G C V I A W N S N N L D S K V G G N Y N	450
EMBOSS_001	451	YLYR L F R K S N L K P F E R D I S T E I Y Q A G S T P C N G V E G F N C Y F P L Q S Y G F Q P T	500
EMBOSS_001	501	NGVGYQP Y R V V V L S <b>FELLH</b> A P A T V C G P K K S T N L V K N K C V N F N F N G L T G T G	550
EMBOSS_001	551	VLTESNKKFLPFQ Q F G R D I A D T T D A V R D P Q T L E I L D I T P C S F G G V S V I T P	600
EMBOSS_001	601	GTNTSNQVAVLYQDVNCTEVPVAI H A D Q L T P T W R V Y S T G S N V F Q T R A G C L	650
EMBOSS_001	651	IGA E H V N N S Y E C D I P I G A G I C A S Y Q T Q T N S P R R A R S V A S Q S I I A Y T M S L G	700
EMBOSS_001	701	AENSVAYSNN S I A I P T N F T I S V T T E I L P V S M T K T S V D C T M Y I C G D S T E C S	750
EMBOSS_001	751	NLL L Q Y G S F C T Q L N R A L T G I A V E Q D K N T Q E V F A Q V K Q I Y K T P P I K D F G G F	800
EMBOSS_001	801	NFSQILPDPSPKPSKRSFIEDLLFNKVTLADAGFIKQYGDCLGDI AARDLI	850
EMBOSS_001	851	CAQKFNGLTVLPPLLTDEMIAQYTSALLAGTITSGWTFGAGAALQIPFAM	900
EMBOSS_001	901	QMAYRFNGIGVTQNVLYENQKLIANQFN SAIGKIQDSLSTASALGKLQD	950

EMBOSS_001	951	VVNQNAQALNTLVKQLSSNFGAISSVLNDIILSRLDKVEAEVQIDRLITGR	1000
EMBOSS_001	1001	LQSLQTYVTQQLIRAAEIRASANLAATKMSECVLQSKRVDFCGKGYHLM	1050
EMBOSS_001	1051	SFPQSAPHGVVFLHVITYVPAQEKNFTTAPAICHGKAHFPREGVVFVSNGT	1100
EMBOSS_001	1101	HWFVTQRNFYEQIITTDNTFVSGNCDVVIGIVNNTVYDPLQPELDSFKE	1150
EMBOSS_001	1151	ELDKYFKNHTSPDVDLGDISGINASVVNIQKEIDRLNEVAKNLNESLIDL	1200
EMBOSS_001	1	-----MMPVILLLLLS----LAIRCAD	18
		::: ...    ... ..	
EMBOSS_001	1201	QELGKYEQYIKWPWYIWLGFIAGLIAIVMVTIMLCCMTSCCCLKGCCSC	1250
EMBOSS_001	19	GKAVQGSDSPASLLTGDKNHDLPVKRDCTTCAGEECCGRCTCPWGDNCS	68
		...:. ... .:. ... .:. ...	
EMBOSS_001	1251	GSCCKFDEDDSEPVLLKGVKLHYT-----	1273
EMBOSS_001	69	<b>CIEWGK</b> 74	
EMBOSS_001	1274	-----  1273	

Protein Sequence Alignment between SARS-CoV-2 spike glycoprotein (GenBank: NC\_045512.2) and Conotoxin Cal5a L3, *Californiconus californicus* (*California cone*) (*Conus californicus*) (UniProtKB: D2YI69 - CU51C\_CONCL) protein.

MRFYIGLMAALMLTSVLRDTSASVGQTGKSELAVIERVIRQRDAADV KPVARQNEGPGRDPAPCCQHPIETCCRR

EMBOSS_001	1	MFVFLVLLPLVSSQCVNLTTRTQLPPAYTNSFTRGVYYPDKVFRSSVLHS	50
EMBOSS_001	51	TQDLFLPFFSNVTWFHAIHVSGTNGTKRFDNPVLPFNDGVYFASTEKSNI	100
EMBOSS_001	101	IRGWIFGTTLDSKTQSLLIIVNATNVVIKVFCEQFCNDPFLGVYHKNK	150
EMBOSS_001	151	SWMESEFRVYSSANNCTFEYVSQPFLMDLEGKQGNFKNLREFVFNIDGY	200
EMBOSS_001	201	FKIYSKHTPINLVRDLPQGFSALEPLVDLPIGINITRFQTLALHRSYLT	250
EMBOSS_001	251	PGDSSSGWTAGAAAYVGYLQPRTFLLKYNENGTITDAVDCALDPLSETK	300
EMBOSS_001	301	CTLKSFTVEKGIYQTSNFRVQPTESIVRFPNITNLCPFGEVFNATRFASV	350
EMBOSS_001	351	YAWNKRKISNCVADYSVL <b>YNSASSTFKCYGVSPTKLN</b> DL	400
		CFITNVYADSF	
EMBOSS_001	401	VIRGDEVQRQIAPGQTGKIADYNYKLPDDEFTGCVIAWNSNLDKVVGGNYN	450
EMBOSS_001	451	YLYRLFRKSNLKPFRDISTEIYQAGSTPCNGVEGFNCYFPLQSYGFQPT	500
EMBOSS_001	501	NGVGYQPYRVVLS <b>FELLH</b> APATVCGPKKSTNLVKNKCVNFNGLTGTTG	550
EMBOSS_001	551	VLTESNKKFLPFQQFGRDIADTTDAVRDPQTLLEILDITPCSFGGVSVITP	600
EMBOSS_001	601	GTNTSNQVAVLYQDVNCTEVVPAIHADQLTPTWRVYSTGSNVFQTRAGCL	650
EMBOSS_001	651	IGAETHVNSYECDIPIGAGICASYQTQTNPRRARSVASQSIAYTMSLG	700
EMBOSS_001	701	AENSVAYSNNNSIAIPTNFTISVTTEILPVSMKTSVDCTMYICGDSTEC	750
EMBOSS_001	751	NLLQYGSFCTQLNRALTGIAVEQDKNTQEVFAQVKQIYKTPPIKDFGGF	800
EMBOSS_001	801	NFSQILPDPKSKRSFIEDLLFNKVTLADAGFIKQYGDCLGDIARDLI	850
EMBOSS_001	851	CAQKFNGLTVLPLLTDDEMIAQYTSALLAGTITSGWTFGAGAALQIPFAM	900
EMBOSS_001	901	QMAYRFNGIGVTVQNVLYENQKLIANQFNSAIGKIQDSLSTASALGKLQD	950

```

EMBOSS_001      951 VVNQNAQALNTLVKQLSSNFGAISSVLNDILSRDKVEAEVQIDRLITGR      1000
EMBOSS_001      1001 LQSLQTYVTQQLIRAAEIRASANLAATKMSECVLGQSKRVDFCGKGYHLM      1050
EMBOSS_001      1051 SFPQSAPHGVVFLHVTVYPAQEKNFHTTAPAICHGDKAHFPREGVFFVSNGT      1100
EMBOSS_001      1101 HWFVTQRNFYEQIITTDNTFVSGNCDVVIGIVNNTVYDPLQPELDSFKE      1150
EMBOSS_001      1151 ELDKYFKNHTSPDVDLGDISGINASVVNIQKEIDRLNEVAKNLNESLIDL      1200
EMBOSS_001           1 -----MRFYIGLMAALMLTSVLRRTDSASVGQTGTKSEL           33
EMBOSS_001      1201 QELGKYEQYIKWPWYIWLGFIAGLIAIVMVTIML-----              1234
EMBOSS_001           34 AVIERVIRQRDAADV KPVARQNEGPGRDPAPCCQHPIETCCRR-----           76
EMBOSS_001      1235 -----CC---MTSCCSCCLKGCCSC              1250
EMBOSS_001      1251 GSCCKFDEDDSEPV LKGVKLYHT      1273
    
```

Protein Sequence Alignment between SARS-CoV-2 spike glycoprotein (GenBank: NC\_045512.2) and **Alpha-conotoxin CIB**, *Conus catus* (*Cat cone*) (UniProtKB: P0DPT2 - CA1B\_CONCT) protein.

SDGRNEAANDEASDVIELALKGCCSNPVCHLEHPNACGRRR

```

EMBOSS_001           1 MFVFLVLLPLVSSQCVNLTTRTQLPPAYTNSFTRGVYYPDKVFRSSVLHS           50
EMBOSS_001           51 TQDLFLPFFSNVTWFHAIHVSQGTNGTKRFDNPVLPFNDGVYFASTEKSNI           100
EMBOSS_001          101 IRGWIFGTTLDSTQSLIVNATNVVIKVFCEQFCNDPFLGVYYHKNNK           150
EMBOSS_001          151 SWMESEFRVYSSANNCTFEYVSQPFLMDLEGKQGNFKNLREFVFKNIDGY           200
EMBOSS_001          201 FKIYSKHTPINLVRDLPOGFSALEPLVDLPIGINITRFQTLALHRSYLT           250
EMBOSS_001          251 PGDSSSGWTAGAAAYVGYLQPRTFLLKYNENGTITDAVDCALDPLSETK           300
EMBOSS_001          301 CTLKSFTVEKGIYQTSNFRVQPTESIVRFPNITNLCPFGEVFNATRFASV           350
EMBOSS_001          351 YAWNKRKISNCVADYSVLYNSASFSTFKCYGVSPTKLNDLCFTNVYADSF           400
EMBOSS_001          401 VIRGDEVQRQIAPGQTGKIADYNYKLPDDEFTGCVIAWNSNNLDSKVGGNYN           450
EMBOSS_001          451 YLYRFLFRKSNLKPFFERDISTEIYQAGSTPCNGVEGFNCYFPLQSYGFQPT           500
EMBOSS_001          501 NGVGYQPYRVVLSFELLHAPATVCGPKKSTNLVKNKCVNFNFNGLTGTG           550
EMBOSS_001          551 VLTESNKKFLPFQQFGRDIADTTDAVRDPQLEILDITPCSFGGVSVITP           600
EMBOSS_001          601 GTNTSNQVAVLYQDVNCTEVPVAIHADQLTPTRVYSTGSNVFQTRAGCL           650
EMBOSS_001          651 IGAEHVNNSEYCDIPIGAGICASYQTQTNPRRARSVASQSIAYTMSLG           700
EMBOSS_001          701 AENSVAYSNNSIAIPTNFTISVTTEILPVSMKTTSVDCTMYICGDSTECS           750
EMBOSS_001          751 NLLLYGSGFCTQLNRALTGIAVEQDKNTQEVFAQVKQIYKTPPIKDFGGF           800
EMBOSS_001          801 NFSQILPDPSKPSKRSFIEDLLFNKVTLADAGFIKQYGDCLGDIAARDLI           850
EMBOSS_001          851 CAQKFNGLTVLPELLTDEMIAQYTSALLAGTITSGWTFGAGAALQIPFAM           900
EMBOSS_001          901 QMAYRFNGIGVTVQNVLYENQKLIANQFNSAIGKIQDSLSSTASALGKLQD           950
    
```

EMBOSS_001	951	VVNQNAQALNTLVKQLSSNFGAISSVLNDILSRDKVEAEVQIDRLITGR	1000
EMBOSS_001	1001	LQSLQTYVTQQLIRAAEIRASANLAATKMSECVLGQSKRVDFCGKGYHLM	1050
EMBOSS_001	1051	SFPQSAPHGVVFLHVITYVPAQEKNFTTAPAICHGKAHFPREGVVFVSNGT	1100
EMBOSS_001	1101	HWFVTQRNFYEQIITTDNTFVSGNCDVVIGIVNNTVYDPLQPELDSFKE	1150
EMBOSS_001	1	-----SDGRNEAA-----NDEASDV	15
EMBOSS_001	1151	ELDKYFKNHTSPDVDLGDISGINASVVNIQKEIDRLNEVAKNLNESLIDL	1200
EMBOSS_001	16	IEL-----ALKGCCSN	26
EMBOSS_001	1201	QELGKYEQYIKWPWYIWLGFIAGLIAIVMVTIMLCCMTSCCSCCLKGCCS-	1249
EMBOSS_001	27	PVCHLEHPNACGRRR-----41	
EMBOSS_001	1250	-----CGSCCKFDEDDSEPVLKGVKLHYT	1273

Protein Sequence Alignment between SARS-CoV-2 spike glycoprotein (GenBank: NC\_045512.2) and **Kunitz-type serine protease inhibitor conotoxin Cal9.1a**, *Californiconus californicus* (*California cone*) (*Conus californicus*) (UniProtKB: D2Y488 - VKT1A\_CONCL) protein.

MTFLLLLVSVCMMATGEERTKRDVCELPEEGPCFAAIRVYAYNAETGDCEQLTYGGCEGNGNRFATLED CDNACARY

EMBOSS_001	1	MFVFLVLLPLVSSQCVNLTTRTQLPPAYTNSFTRGVYYPDKVFRSSVLHS	50
EMBOSS_001	51	TQDLFLPFFSNVTWFHAIHVSGTNGTKRFDNPVLPFNDGVYFASTEKSNI	100
EMBOSS_001	101	IRGWIFGTTLDSKTQSLIVN NATNVVIKVFCEQFCNDPFLGVYYHKNNK	150
EMBOSS_001	151	SWMESEFRVYSSANNCTFEYVSQPFLMDLEGKQGNFKNLREFVFKNIDGY	200
EMBOSS_001	201	FKIYSKHTPINLVRDLPQGFSALEPLVDLPIGINITRFQTLALHRSYLT	250
EMBOSS_001	251	PGDSSSGWTAGAAAYVGYLQPRTFLLKYNENGTITDAVDCALDPLSETK	300
EMBOSS_001	301	CTLKSFTVEKGIYQTSNFRVQPTESIVRFPNITNLCPFGEVFNATRFASV	350
EMBOSS_001	351	YAWNRKRISNCVADYSVL <b>YNSASF</b> <span style="border: 1px solid red; padding: 2px;">STFKCYGVSPTKLNDL</span> CFTNVYADSF	400
EMBOSS_001	401	VIRGDEVQRQIAPGQTGKIADYNYKLPD <b>DF</b> TGCVIAWNSNLLDSKVGGNYN	450
EMBOSS_001	451	YLYRFLFRKSNLKPFERDISTEYIYQAGSTPCNGVEGFNCYFPLQSYGFQPT	500
EMBOSS_001	501	NGVGYQPYRVVLS <b>FELL</b> HAPATVCGPKKSTNLVKNKCVNFNFNGLTGTG	550
EMBOSS_001	1	-----MTFLLLLVSVC-----MMATG	16
EMBOSS_001	551	VLTESNKKFLPFQQFGRDIADTTDAVRDPQTL EILDITPCSEFGGVSVITP	600
EMBOSS_001	17	EERTKRDVCELPEEGPCF-----AAI-----RVYAYNAETGDCEQLT	54
EMBOSS_001	601	GTNTSNQVAVL-YQDVNCTEVPVAIHADQLTPTWRVYS-----TGSNVFQT	645
EMBOSS_001	55	YGGCEGNGNRFATLED <b>CD</b> -----NACARY-----	78
EMBOSS_001	646	RAGCLIGAEHVNSYECDIPIGAGICASYQTQTNSPRRARSVASQSIIAY	695
EMBOSS_001	696	TMSLGAENSVAYSNNISIAIPTNFTISVTTEILPVSMTKTSVDCTMYICGD	745
EMBOSS_001	746	STECSNLLLQYGSFCTQLNRALTGIAVEQDKNTQEVFAQVKQIYKTPPIK	795
EMBOSS_001	796	DFGGFNFSQILPDPSPKSKRSFIEDLLFNKVTLADAGFIKQYGDCLGDIA	845

EMBOSS_001	846	ARDLICAQKFNGLTVLPPLLTDEMIAQYTSALLAGTITSGWTFGAGAALQ	895
EMBOSS_001	896	IPFAMQMAYRFNGIGVTONVLYENQKLIANQFNSAIGKIQDLSLSTASAL	945
EMBOSS_001	946	GKLQDVVNQNAQALNTLVKQLSSNFGAISSVLNDILSRDKVEAEVQIDR	995
EMBOSS_001	996	LITGRLOSLQTYVVTQQLIRAAEIRASANLAATKMSECVLGQSKRVDFCGK	1045
EMBOSS_001	1046	GYHLMSFPQSAPHGVVFLHVTVVPAQEKNFTTAPAICHDKAHFPREGVF	1095
EMBOSS_001	1096	VSNGTHWFVTQRNFYEQIITTDNTFVSGNCDVVIGIVNNTVYDPLQPEL	1145
EMBOSS_001	1146	DSFKEELDKYFKNHTSPDVLGDISGINASVVNIQKEIDRLNEVAKNLNE	1195
EMBOSS_001	1196	SLIDLQELGKYEQYIKWPWYIWLGFIAGLIAIVMVTIMLCCMTSCCCLK	1245
EMBOSS_001	1246	GCCSCGSCCKFEDEDDSEPVKGVKLVHYT 1273	

Protein Sequence Alignment between SARS-CoV-2 spike glycoprotein (GenBank: NC\_045512.2) and Alpha-conotoxin-like Qc1.2, *Conus quercinus* (Oak cone) (UniProtKB: Q6PTD6 - CA12\_CONQU) protein.

MGMRMMFTVFLVALATTVASFTLDRASNGRNAAADDKPSDWIALAIKQCCANPPCKHVNCR

EMBOSS_001	1	MEVFLVLLPLVSSQCVNLTTRTQLPPAYTNSFTRGVYYPDKVFRSSVLHS	50
EMBOSS_001	51	TQDLFLPFFSNVTWFHAIHVSGTNGTKRFDNPVLPFNDGVYFASTEKSN	100
EMBOSS_001	101	IRGWIFGTTLDSKTQSLIIVNATNVVIKVEFCNDPFLGVYHKNK	150
EMBOSS_001	151	SWMESEFRVYSSANNCTFEYVSQPFLLMDLEKQGNFKNLREVFKNIDGY	200
EMBOSS_001	201	FKIYSKHTPINLVRDLPGFSALEPLVDLPIGINITRFQTLALHRSYLT	250
EMBOSS_001	251	PGDSSSGWTAGAAAYVGYLQPRTFLLKYNENGTITDAVDCALDPLSETK	300
EMBOSS_001	301	CTLKSFTVEKGIYQTSNFRVQPTESIVRFPNITNLCPFGEVFNATRFASV	350
EMBOSS_001	351	YAWNRKRISNCVADYSVL <del>YNSASESTFKCYGVSPTKLN</del> DL <del>CF</del> TNVYADSF	400
EMBOSS_001	401	VIRGDEVQRQIAPGQTGKIADYNYKLPDDFTGCVIAWNSNNLDSKVGNYN	450
EMBOSS_001	451	YLYRFLFRKSNLKPFFERDISTEIQAGSTPCNGVEGFNCYFPLQSYGFQPT	500
EMBOSS_001	501	NGVGYQPYRVVLS <del>FELL</del> HAPATVCGPKKSTNLVKNKCVNFFNGLTGTG	550
EMBOSS_001	551	VLTESNKKFLPFQFGRDIADTTDAVRDPQTLIILDITPCSFGGVSVITP	600
EMBOSS_001	601	GTNTSNQVAVLYQDVNCTEVPVAIHADQLTPTRVYSTGSNVFQTRAGCL	650
EMBOSS_001	651	IGAHEVNNSYECDIPIGAGICASYQTQTNPRRARSVASQSIAYTMSLG	700
EMBOSS_001	1	-----MGMRMMFTV-----FLLVALATTVASFT-----	23
EMBOSS_001	701	AENSVAYSNNIAIPTNFTISVTEILPVSMTKTSVDCTMYICGDSTEC	750
EMBOSS_001	24	-----LDRASNGRNAAADDKPSDWIALAIKQCCANPPCKHVNC	61
EMBOSS_001	751	-----NLLLQYGSFCTQLNRALTG-IAVEQDKNTQEVFAQVKQIYKTPPIKDFGG	799
EMBOSS_001	62	R-----	62
EMBOSS_001	800	FNFSQILPDPSKPSKRSFIEDLLFNKVTLADAGFIKQYGDCLGDIARDL	849





EMBOSS_001	947	KLQDVVNQNAQALNTLVKQLSSNFGAISSVLNDILSRLDKVEAEVQIDRL	996
EMBOSS_001	997	ITGRLQSLQTYVTQQLIRAAEIRASANLAATKMSECVLGQSKRVDFCGKG	1046
EMBOSS_001	1047	YHLMSFPQSAPHGVVFLHVTYVPAQEKNFTTAPAICHDKGAHFPREGVFFV	1096
EMBOSS_001	1097	SNGTHWFVTQRNFYEQIITTDNTFVSGNCDVVIGIVNNTVYDPLQPELD	1146
EMBOSS_001	1147	SFKEELDKYFKNHTSPDVDLGDISGINASVVNIQKEIDRLNEVAKNLNES	1196
EMBOSS_001	1197	LIDLQELGKYEQYIKWPWYIWLGFIAGLIAIVMVTIMLCCMTSCCCLKG	1246
EMBOSS_001	1247	CCSCGSCCKFDEDDSEPVKLGVKLHYT	1273

Protein Sequence Alignment between SARS-CoV-2 spike glycoprotein (GenBank: NC\_045512.2) and Conotoxin Bu22, *Conus bullatus* (*Bubble cone*) (UniProtKB: P0CY77 - CA122\_CONBU) protein.

SDRASDGRNAAANDRASDLVALTVRGCCTYPPCAVLSPLCD

EMBOSS_001	1	MFVFLVLLPLVSSQCVNLTTRTQLPPAYTNSFTRGVYYPDKVFRSSVLHS	50
EMBOSS_001	51	TQDLFLPFFSNVTWFHAIHVSGTNGTKRFDNPVLPFNDGVYFASTEKSNI	100
EMBOSS_001	101	IRGWIFGTTLDSKTQSLLIIVNNATNVVIKVCDFQFCNDPFLGVYYHKNNK	150
EMBOSS_001	151	SWMESEFRVYSSANNCTFEYVSQPFLMDLEGKQGNFKNLREFFVKRIDGY	200
EMBOSS_001	201	FKIYSKHTPINLVRDLPQGFSALEPLVDLPIGINITRFQTLALHRSYLT	250
EMBOSS_001	251	PGDSSSGWTAGAAAYVGYLQPRTFLLKYNENGTITDAVDCALDPLSETK	300
EMBOSS_001	301	CTLKSFTVEKGIYQTSNFRVQPTESIVRFPNITNLCPFGEVFNATRFASV	350
EMBOSS_001	351	YAWNKRKISNCVADYSVL <b>YNSASESTFKCYGVSPTKLNDL</b> CFTNVYADSF	400
EMBOSS_001	401	VIRGDEVQRQIAPGQTGKIADYNYKLPDDFTGCVIAWNSNNLDSKVGGNYN	450
EMBOSS_001	451	YLYRLFRRKSNLKPFFERDISTEYIYQAGSTPCNGVEGFNCYFPLQSYGFQPT	500
EMBOSS_001	501	NGVGYQPYRVVLS <b>FELLH</b> APATVCGPKKSTNLVKNKCVNFNGLTGTG	550
EMBOSS_001	551	VLTESNKKFLPFQQFGRDIADTTDAVRDPQTLLEILDITPCSFGGVSVITP	600
EMBOSS_001	601	GTNTSNQVAVLYQDVNCTEVPVAIHADQLTPTRVYSTGSNVFQTRAGCL	650
EMBOSS_001	651	IGAHEVNNSYECDIPIGAGICASYQTQTNSPRRARSVASQSI IAYTMSLG	700
EMBOSS_001	701	AENSVAYSNNSIAIPTNFTISVTTEILPVSMTKTSVDCTMYICGDSTEC	750
EMBOSS_001	751	NLLQYGSFCTQLNRALTGIAVEQDKNTQEVFAQVKQIYKTPPIKDFGGF	800
EMBOSS_001	801	NFSQILPDPSKPSKRSFIEDLLFNKVTLADAGFIKQYGDCLGDI AARDLI	850
EMBOSS_001	851	CAQKFNGLTVLPLLTDemiaQYTSALLAGTITSGWTFGAGAALQIPFAM	900
EMBOSS_001	901	QMayRFNGIGVTQNVLYENQKLIANQFNsaIGKIQDslsStASALgKlQD	950
EMBOSS_001	951	VVNQNAQALNTLVKQLSSNFGAISSVLNDILSRLDKVEAEVQIDRLITGR	1000
EMBOSS_001	1001	LQSLQTYVTQQLIRAAEIRASANLAATKMSECVLGQSKRVDFCGKGYHLM	1050
EMBOSS_001	1051	SFPQSAPHGVVFLHVTYVPAQEKNFTTAPAICHDKGAHFPREGVFFVSNGT	1100

EMBOSS_001	1101	HWFVTQRNFYEPQIITTDNTFVSGNCDVVIGIVNNTVYDPLQPELDSFKE	1150
EMBOSS_001	1	-----SDRASD-GRNAAANDRAS	17
EMBOSS_001	1151	ELDKYFKNHTSPDVDLGDISGINASVVNIQKEIDRLNEVAKN--LNESLI	1198
EMBOSS_001	18	DL-----VALTVRGCCTYPECAVLSPLC	40
EMBOSS_001	1199	DLQELGKYEQYIKWPWYIWLGFIAGLIAIVMVTIMLCMTSCCSCLKGCC	1248
EMBOSS_001	41	D-----	41
EMBOSS_001	1249	SCGSCCKFDEDDSEPVLKGVKLHYT	1273

**A**

**B**

**C**

EMBOSS_001	601	GTNTSNQVAVLYQDVNCTEVPVAIHADQLTPTWRVYSTGSNWFQTRAGCL	650
EMBOSS_001	1	-----	0
EMBOSS_001	651	IGAETHVNSYECDIPIGAGICASYQTQNSPRRARSVASQSIAYTHSLG	700
EMBOSS_001	1	-----MGRMRFMTV-----FLLVALATTVASFT-----	23
EMBOSS_001	701	AENSVAYSNNISIAIPTNFTISVTEILPVSHKTSVDCTHYICGDSTEC	750
EMBOSS_001	24	-----LDRASNGRNAADDKPSDWIALAIKQCCANPPCKHVNC	61
EMBOSS_001	751	NLLQYGSFCTQLNRALTG-IAVEQDKNTQEVFAQVKQIYKTPPIKDFGG	799
EMBOSS_001	61	-----	62
EMBOSS_001	849	EDLLFNKVTLADAGFIKQYGDCLGDTAARDL	849
EMBOSS_001	62	-----	62

(|) = identical amino acids  
 (:) = strongly conserved amino acids  
 (.) = weakly conserved amino acids

**Supplementary Figure 1.** Simplified schematic representation of the use of the EMBOSS Needle web tool ([https://www.ebi.ac.uk/Tools/psa/emboss\\_needle/](https://www.ebi.ac.uk/Tools/psa/emboss_needle/)) for protein sequence alignment and comparison. A: Step 1 - Input Sequences. In this step, the software requests the input of the two protein sequence sequences to be compared represented by a free (raw) text list of a block of characters retrieved from the Protein Sequence Databases. In this case, the sequence of SARS-CoV-2 spike glycoprotein (GenBank: NC\_045512.2) and Alpha-conotoxin-like Qc1.2, *Conus quercinus* (Oak cone) (UniProtKB: Q6PTD6 - CA12\_CONQU) protein are compared. B: Step 2 - Set alignment and output file options and submit. In this step it is possible to set some calculation options to the algorithm according to the needs of the bioinformatics analysis to be performed. It is also possible to choose a specific output format of the results file according to the needs of the study. C: Output file with the results of the comparison of the analyzed protein sequences. Identical amino acids are connected with a “[” symbol, strongly similar amino acids are connected with a “:” symbol and weakly similar ones are indicated with “.”.